Supplementary Information (SI) for Journal of Materials Chemistry B.

Ultra-photostable fluorescent dye molecular engineering—for measuring plant cells' membrane-spacing through "deposition-embedding" strategy

Wendong Jin,[a] Jie Huang,[a] Jie Niu,[b] Shiqian Zhang,[a] Zhiqiang Liu *[a], Xiaoqiang Yu*[a]

[a]State Key Laboratory of Crystal Materials, Shandong University, Jinan 250100, China.

[b]Department of Otolaryngology-Head and Neck Surgery, Shandong Institute of Otorhinolaryngology, Shandong Provincial ENT Hospital, Shandong University, Jinan 250022, China.

E-mail: zqliu@sdu.edu.cn; yuxq@sdu.edu.cn

1. Experimental Section

Materials and General Information:

All reactants and solvents, unless otherwise stated, were purchased from commercial sources and used as received. Flash chromatography was carried out on silica gel (200-300 mesh).

400MHz ^{1}H NMR and 100MHz ^{13}C NMR spectra were recorded on a Bruker spectrometer. Chemical shifts were expressed in ppm and coupling constants (*J*) in Hz. High-Res MS (HRMS) were record in MALDI (DHB matrix) or ESI modes.

UV-visible absorption spectra were recorded on a U-2910 Double-beam UV/VIS spectrophotometer. The fluorescence data was measured on a F-2700FC spectrophotometer. Fluorescence quantum yields and photoluminescence lifetime were determined on Edinburgh Instruments FLS-980 apparatus.

The suitable crystals for X-ray were grown by slow evaporation from their hexane or hexane/DCM solution. The suitable each crystal was mounted on a nylon loop using a small amount of Paratone N oil. All X-ray measurements were carried on a Bruker SMART diffractometer equipped with a graphite monochromated Cu Ka (λ = 1.54184 Å) radiation source and a CCD detector at 173 K. The frame integration was performed using the program SAINT. The structures were solved by direct method provided by the program package Olex2 and refined a full matrix least square against F2 for all data. All non-hydrogen atoms were refined anisotropically. Absorption correction were applied based on multiple and symmetry-equivalent measurements. The hydrogen atoms were included in the models in calculated positions and were refined as constrained to bonding atoms. CCDC:2389313 (PTBT-H), 2361154 (PTBT-NPh_2) and 2361155 (PTBT-O-NPh_2) contains the supplementary crystallographic data for this paper.

Theoretical Calculations:

Geometry optimizations were performed using the Gaussian 09 program at the B3LYP/6-31+G(d) level of theory. The optimized geometries at the same level were employed for the TD-DFT calculations at the B3LYP/6-31+ G (d) level of theory. For estimation of the NICS (nucleus-independent chemical shift) values of 2, GIAO calculations were performed at the HF/6-31+G (d, p) level using the optimized geometry.

Cell culture and imaging:

HeLa cells were obtained from the Experimental Animal Center of Shandong University. Cells were cultured in H-DMEM supplemented with 10 % fetal bovine serum (FBS) and 1 % penicillin and streptomycin. All of the above cells were cultured in a 5 % CO2 incubator at 37 °C. Before cell staining, all cells were plated on glass coverslips and allowed to adhere for 24 h. Fresh H-DMEM medium containing 10 μM of PTBT-O-NPh_2 was added to the culture medium of HeLa cells and incubated for 80min before imaging. For co-stain imaging, the HeLa cells were incubated with 2 μM Bodipy 493/503 for 20 min and 5 μM hochest33342 for 30 min.

For plant cell imaging, PBS buffer was used as the cell survival environment. The probe staining concentration is 20 μM of DiD and PTBT-O-NPh_2.

Confocal fluorescence imaging was obtained on Olympus FV 1200 laser confocal microscope.

Two-photon fluorescence spectroscopy acquisition

The two-photon fluorescence test was performed by a Ti:Sapphire Mira 900-F femtosecond laser with a pulsed laser light source of 130 fs pulses and a repetition rate of 76 MHz, and the data was recorded with a Spectro Pro 300 i spectrometer. The standard dye Rho B was used as a reference to measure the two-photon absorption cross-sections of the two compounds. The calculation equation was estimated as,

$$\delta_{sam} = \delta_r \times \frac{\Phi_{ref} c_{ref} n_{ref} F_{sam}}{\Phi_{sam} c_{sam} n_{sam} F_{ref}}$$

where δ_{sam} and δ_{ref} is the two-photon absorption cross-section of samples and reference. c_{sam} and c_{ref} are the concentration of sample and reference (10 μM). n_{sam} and n_{ref} are the refractive indices of their respective solvents. F_{sam} and F_{ref} are the fluorescence integration intensity of two-photon excitation.

Table S1 Summary of plant cell membrane probes

Probes	Abs/Em	Staining conditions	Stained Results
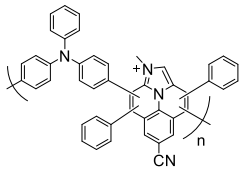 ACS Applied Materials & Interfaces (DOI: 10.1021/acsami.3c16257)	410nm/618nm	staining concentration =10 μM, staining time =20 min. λex =405 nm, λem =600-800 nm.	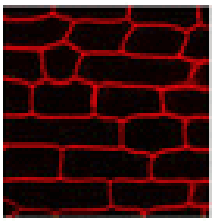
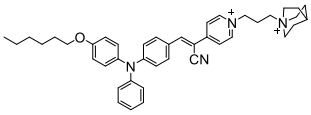 Chemical Science (DOI: 10.1039/d2sc05727a)	525nm/660nm	staining concentration =10 μM, staining time =5 min. λex=543nm, λem=600-700nm.	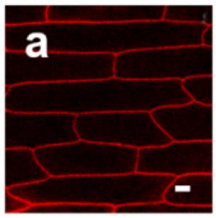
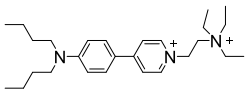 Biosensors and Bioelectronics (10.1016/j.bios.2024.117039)	450nm/520nm	staining concentration =10 μM, staining time =5 min. λex =473 nm, λem =500-600 nm.	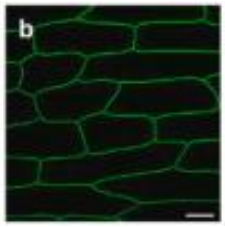
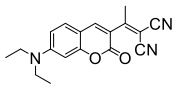 Photochemical & Photobiological Sciences (10.1007/s43630-024-00637-z)	460nm/560nm	staining concentration =10 μM, staining time =8 h. λex =570 nm, λem =590-640 nm.	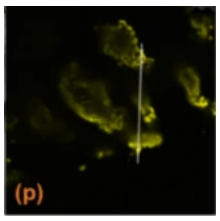
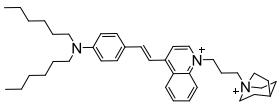 Journal of Materials Chemistry B (10.1039/d3tb02601a)	600nm/700nm	staining concentration =10 μM, staining time =20min. λex =633 nm, λem =650-750 nm.	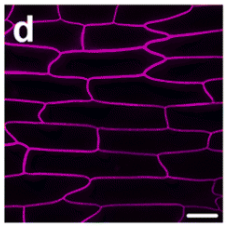

2. Synthetic procedures

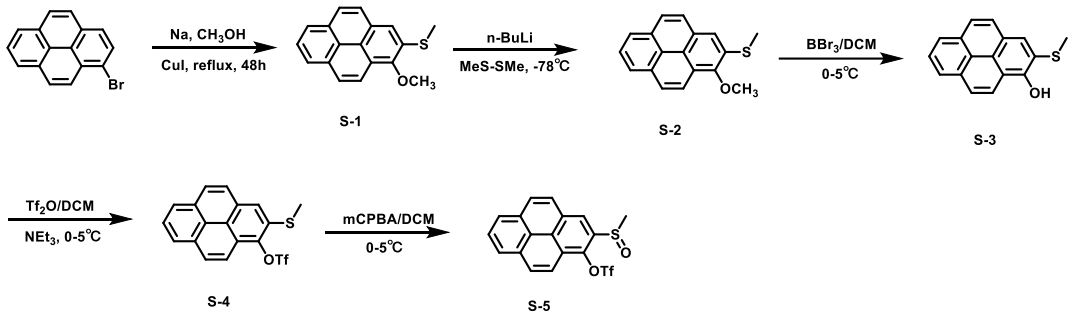

Scheme S1 The synthesis route of the compound S-5

Synthesis of S-1: 1-bromopyrene (2.53 g, 9 mmol) and CuI (0.19 g, 1 mmol) were added to the fresh sodium methylate solution, which by adding Na (1.43 g) into methanol (17.5 mL) under the atmosphere of nitrogen. Then, DMF (7 mL) was added into the mixture. The mixture was then stirred at 90 ℃ for 48 h. The solvent was evaporated and the residue was purified by silica gel column chromatography using dichloromethane/hexane as eluent to obtain white powder of S-1. Yield: 1.75 g (84 %) ^{1}H NMR ($CDCl_3$, 400 MHz) δ (ppm): 8.46 (d, J = 9.2 Hz, 1H), 8.14 – 8.04 (m, 4H), 7.99 – 7.94 (m, 2H), 7.89 (d, J = 8.9 Hz, 1H), 7.56 (d, J = 8.4 Hz, 1H), 4.18 (s, 3H). ^{13}C NMR ($CDCl_3$,101 MHz) δ (ppm): 153.69, 131.80, 131.73, 127.30, 126.43, 126.15, 125.84, 125.53, 125.27, 125.01, 124.99, 124.29, 124.20, 121.17, 120.25, 108.08, 56.16. MS (mass m/z): calcd for $C_{17}H_{12}OH^+$ [M+H] $^+$ 233.0961, found for $C_{17}H_{12}OH^+$ [M+H] $^+$.233.0960

Synthesis of S-2: S-1 (2.3 g, 10 mmol) was added to the dry Tetrahydrofuran solution, then KOt-Bu (1.2 g, 12 mmol) and 2,2,6,6-Tetramethylpiperidine (1.6 g, 12 mmol) were added to the mixture. And then the mixture was cooled down to -78 ℃, followed by slow addition of 12.8 mL (20 mmol, 1.6 M in Hexane) of a solution of n-butyllithium in hexane. After addition, the mixture turned yellow. After 50min of stirring, at a constant temperature, Dimethyl disulfide (1.6 g, 10 mmol) was added to the mixture. After slowly rising to room temperature, 20 mL of water was added to the solution and the organic layer was separated, whereas the aqueous layer was extracted two times with 50 mL of ethyl acetate. Then, combined extracts were dried over Na_2SO_4. The solvent was evaporated and the residue was purified by silica gel column chromatography using dichloromethane/hexane as eluent to obtain white powder of S-2. Yield: 1.76 g (64 %) ^{1}H NMR ($CDCl_3$, 400 MHz) δ (ppm):

8.27 (d, J = 9.2 Hz, 1H), 8.14 (d, J = 7.6 Hz, 2H), 8.09 (d, J = 9.2 Hz, 1H), 8.03 – 7.93 (m, 4H), 4.12 (s, 3H), 2.70 (s, 3H). ^{13}C NMR ($CDCl_3$,101 MHz) δ (ppm): 150.85, 130.73, 128.50, 126.91, 126.43, 125.83, 125.22, 125.04, 124.80, 123.93, 123.66, 121.57, 120.84, 61.70, 14.99. MS (mass m/z): calcd for $C_{18}H_{14}OSH^+$ [M+H] $^+$ 279.0838, found for $C_{18}H_{14}OSH^+$ [M+H] $^+$ 279.0840.

Synthesis of S-3: Boron tribromide (7.2 g, 28.7 mmol) was added to the dry dichloromethane solution (30 mL), and then the mixture was cooled down to 0-5 ℃. Then, S-2 (1.8 g, 6.5 mmol) was added into the mixture. And then the mixture was stirred at 0-5 ℃ overnight. Then 20 mL of water was added to the solution and the organic layer was separated, whereas the aqueous layer was extracted two times with 50 mL of ethyl acetate. Then, combined extracts were dried over Na_2SO_4. The solvent was evaporated and the residue was purified by silica gel column chromatography using dichloromethane/hexane as eluent to obtain white powder of S-3. Yield: 1.7 g (99 %) ^{1}H NMR ($CDCl_3$, 400 MHz) δ (ppm): 8.27 (d, J = 7.6 Hz, 2H), 8.18 (t, J = 4.5 Hz, 4H), 8.12 (d, J = 9.0 Hz, 2H), 8.04 (t, J = 7.6 Hz, 1H), 2.74 (s, 3H). ^{13}C NMR ($CDCl_3$,101 MHz) δ (ppm): 153.39, 135.98, 135.82, 132.01, 131.70, 131.15, 130.78, 130.09, 129.96, 129.70, 129.45, 129.18, 128.20, 128.02, 126.37, 123.75, 45.32, 45.11, 44.90, 44.69, 44.48, 44.28, 44.07, 20.05. MS (mass m/z): calcd for $C_{17}H_{12}OSH^+$ [M+H] $^+$ 265.0681, found for $C_{17}H_{12}OSH^+$ [M+H] $^+$ 265.0669.

Synthesis of S-4: S-3 (1.3 g, 5 mmol) and TEA (0.6 g, 6 mmol) was added to the dry dichloromethane solution (20 mL), and then the mixture was cooled down to -10 ℃. Then, triflic anhydride (1.7 g, 6 mmol) was added into the mixture. And then the mixture was stirred at -10 ℃ overnight. Then 20 mL of water was added to the solution and the organic layer was separated, whereas the aqueous layer was extracted two times with 40 mL of ethyl acetate. Then, combined extracts were dried over Na_2SO_4. The solvent was evaporated and the residue was purified by silica gel column chromatography using dichloromethane/hexane as eluent to obtain light yellow powder of S-4. Yield: 1.71g (88 %) ^{1}H NMR ($CDCl_3$, 400 MHz) δ (ppm) 8.29 – 8.20 (m, 4H), 8.16 – 8.10 (m, 2H), 8.08 – 7.99 (m, 2H), 2.73 (s, 3H). ^{13}C NMR ($CDCl_3$,101 MHz) δ (ppm): 140.08, 131.01, 130.89, 130.46, 130.13, 130.04, 129.03, 126.66, 126.62, 126.30, 125.92, 124.54, 124.31, 123.73,

123.67, 119.52, 17.03. MS (mass m/z): calcd for $C_{18}H_{11}F_3O_3S_2H^+$ [M+H] $^+$ 397.0174, found for $C_{18}H_{11}F_3O_3S_2H^+$ [M+H] $^+$ 397.0176.

Synthesis of S-5: S-4 (0.198 g, 0.5 mmol) and Boron (tri) fluoride etherate (0.55 mL, 4.3 mmol) was added to the dry dichloromethane solution (8 mL), and then the mixture was cooled down to -20 ℃. Then, mCPBA (0.12 g, 0.67 mmol) was added into the mixture. And then the mixture was stirred at -20 ℃ for 2 h. Then 20 mL of water was added to the solution and the organic layer was separated, whereas the aqueous layer was extracted two times with 15 mL of dichloromethane. Then, combined extracts were dried over Na_2SO_4. The solvent was evaporated to obtain light yellow powder of S-5. Yield: 0.2 g (99 %) ^{1}H NMR ($CDCl_3$, 400 MHz) δ (ppm): 8.81 (s, 1H), 8.36 – 8.31 (m, 4H), 8.27 – 8.20 (m, 2H), 8.16 (t, J = 7.7 Hz, 1H), 3.00 (s, 3H). ^{13}C NMR ($CDCl_3$,101 MHz) δ (ppm): 132.56, 131.25, 127.13, 126.36, 126.19, 125.98, 125.08, 123.07, 122.56, 122.38, 122.11, 122.06, 119.93, 118.79, 115.61, 114.88, 72.62, 72.31, 71.99, 38.41. MS (mass m/z): calcd for $C_{17}H_{12}OSH^+$ [M+H] $^+$ 413.0124, found for $C_{17}H_{12}OSH^+$ [M+H] $^+$ 413.0109.

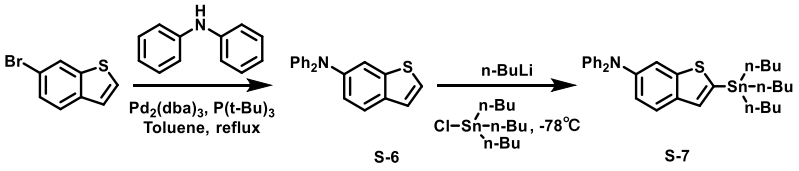

Scheme S2 The synthesis route of the compound S-7

Synthesis of S-6: 6-Bromobenzo[b]thiophene (2.52 g, 11.8 mmol) and Diphenylamine (2 g, 11.8 mmol) were added to the dry toluene solution. Then, KOt-Bu (1.6 g,14.18 mmol), $Pd_2(dba)_3$ (5 % eq) and $P(t\text{-}Bu)_3$ (5 % eq) were added into the mixture. The mixture was then stirred at 120 ℃ for 8 h. The solvent was evaporated and the residue was purified by silica gel column chromatography using dichloromethane/hexane as eluent to obtain white powder of S-6. Yield: 2.4 g (67 %) ^{1}H NMR (DMSO-d_6,400 MHz) δ 7.80 (d, J = 8.6 Hz, 1H), 7.64 (d, J = 5.4 Hz, 1H), 7.59 (d, J = 2.0 Hz, 1H), 7.39 (d, J = 6.2 Hz, 1H), 7.32 – 7.26 (m, 4H), 7.07 (dd, J = 8.6, 2.1 Hz, 1H), 7.05 – 6.98 (m, 6H). ^{13}C NMR (DMSO-d_6,101 MHz) δ (ppm): 144.63, 140.92, 136.06, 129.99, 126.94, 124.85, 124.10, 123.91, 123.23, 122.72, 118.25. MS (mass m/z): calcd for $C_{20}H_{15}NSH^+$ [M+H] $^+$ 302.0998, found $C_{20}H_{15}NSH^+$ [M+H] $^+$ 302.0998.

Synthesis of S-7: S-6 (0.3 g, 1 mmol) was added to the dry Tetrahydrofuran solution, then KOt-Bu (0.12 g, 1.2 mmol) and 2,2,6,6-Tetramethylpiperidine (0.16 g, 1.2 mmol) were added to the mixture. And then the mixture was cooled down to -78 ℃, followed by slow addition of 0.7 mL (1.1 mmol, 1.6 M in hexane) of a solution of n-butyllithium in hexane. After addition, the mixture turned reddish brown. After 50min of stirring, at a constant temperature, tributyltin chloride (0.33 g, 1.1 mmol) was added to the mixture. After slowly rising to room temperature, 20 mL of KF solution was added to the mixture and the organic layer was separated, whereas the aqueous layer was extracted two times with 20 mL of ethyl acetate. Then, combined extracts were dried over Na_2SO_4. The solvent was evaporated to obtain reddish brown oil of S-7. The product was not purified and used directly in the next step.

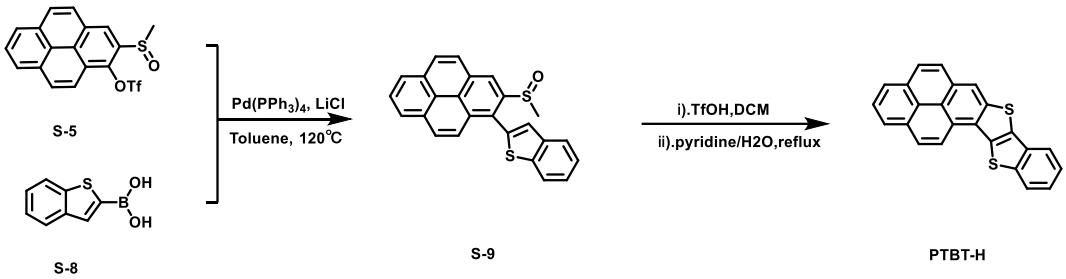

Scheme S3 The synthesis route of the compound PTBT-H

Synthesis of S-9: S-5 (0.2 g, 0.5 mmol) and S-8 (0.11 g, 0.6 mmol) were added to a 10 mL solution of methanol: water: toluene=1:1:1. Then, $Pd(PPh_3)_4$ (10 % eq), and K_2CO_3 (0.23 g, 1.67 mmol) were added into the mixture. The mixture was then stirred at 120 ℃ for 24 h. Then 30 mL of water was added to the mixture and the organic layer was separated, whereas the aqueous layer was extracted two times with 20 mL of ethyl acetate. Then, combined extracts were dried over Na_2SO_4. The solvent was evaporated to obtain reddish brown powder of S-9. The product was not purified and used directly in the next step.

Synthesis of PTBT-H: Trifluoromethanesulfonic acid (1 mL) was added to the flask which contains compound S-9 (0.2 g, 0.5 mmol) in 5 mL of dried DCM. The solution was stirred at room temperature for 24 h, and then poured into a water-pyridine mixture (30mL, 8:1). Demethylation was achieved by reflux for 30 min. After cooling to room temperature, dark red precipitate was collected and washed with water and ethanol. The product was purified by column chromatography using dichloromethane/hexane as eluent to obtain green powder of PTBT-H. Yield: 0.14 g (77.8 %)

^{1}H NMR ($CDCl_3$, 300 MHz) δ (ppm): 8.78 (d, J = 9.0 Hz, 1H), 8.66 (s, 1H), 8.38 (d, J = 9.0 Hz, 1H), 8.29 (d, J = 7.7 Hz, 1H), 8.24 – 8.19 (m, 1H), 8.12 – 7.99 (m, 5H), 7.58 – 7.45 (m, 2H). ^{13}C NMR (101 MHz, Chloroform-d) δ 142.98, 140.67, 134.10, 132.71, 132.64, 131.15, 130.63, 129.34, 128.34, 127.89, 127.66, 127.26, 125.88, 125.52, 125.36, 125.31, 125.12, 125.00, 123.80, 123.61, 122.75, 121.61, 119.87. MS (mass m/z): calcd for $C_{20}H_{15}NSH^{+}$ $[M+H]^{+}$ 365.0453, found for $C_{20}H_{15}NSH^{+}$ $[M+H]^{+}$ 364.0378.

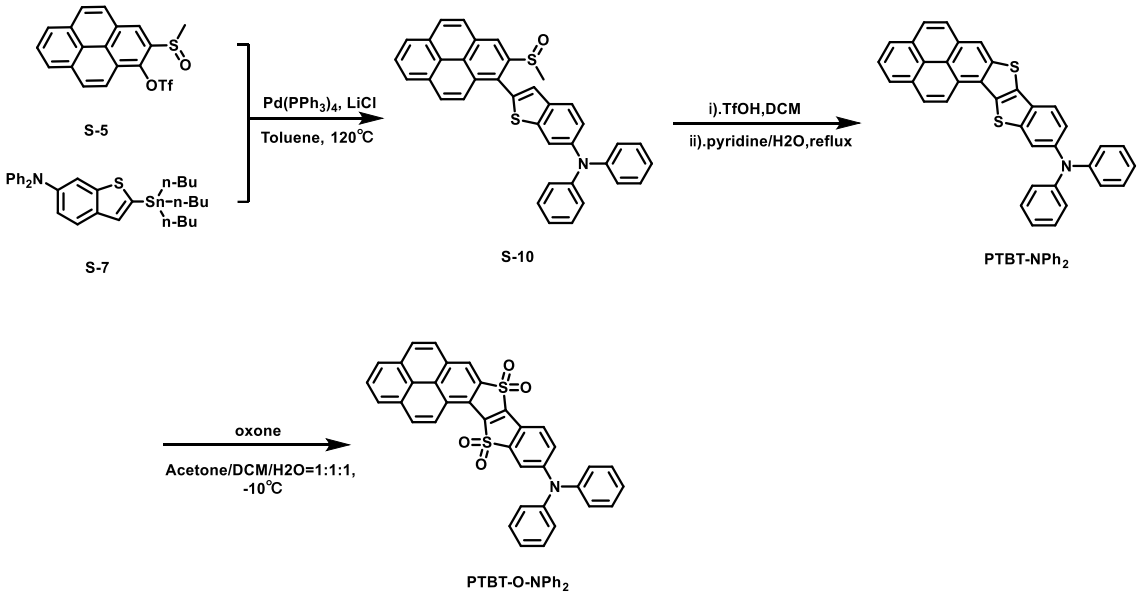

Scheme S4 The synthesis route of the compound PTBT-NPh_2 and PTBT-O-NPh_2

Synthesis of S-10: S-5(0.2 g, 0.5 mmol) and S-7 (0.35 g, 0.6 mmol) were added to the dry toluene solution. Then, $Pd(PPh_3)_4$ (10 % eq), LiCl(0.1 g, 2.3 mmol) and $MgSO_4$(0.2 g, 1.67 mmol) were added into the mixture. The mixture was then stirred at 120 ℃ for 24 h. Then 30 mL of water was added to the mixture and the organic layer was separated, whereas the aqueous layer was extracted two times with 20 mL of ethyl acetate. Then, combined extracts were dried over Na_2SO_4. The solvent was evaporated to obtain reddish brown powder of S-10. The product was not purified and used directly in the next step.

Synthesis of PTBT-NPh_2: Trifluoromethanesulfonic acid (1 mL) was added to the flask which contains compound S-10 (0.28 g, 0.5 mmol) in 5mL of dried DCM. The solution was stirred at room temperature for 24 h, and then poured into a water-pyridine mixture (30 mL, 8:1). Demethylation was achieved by reflux for 30 min. After cooling to room temperature, dark red precipitate was

collected and washed with water and ethanol. The product was purified by column chromatography using dichloromethane/hexane as eluent to obtain green powder of PTBT-NPh_2. Yield: 0.12 g (45.5 %) ^{1}H NMR ($CDCl_3$, 400 MHz) δ (ppm): 8.72 (d, J = 9.0 Hz, 1H), 8.65 (s, 1H), 8.36 (d, J = 9.0 Hz, 1H), 8.28 (d, J = 7.7 Hz, 1H), 8.21 (d, J = 7.5 Hz, 1H), 8.11 – 8.01 (m, 3H), 7.87 (d, J = 8.5 Hz, 1H), 7.70 (d, J = 2.1 Hz, 1H), 7.34 – 7.28 (m, 5H), 7.23 – 7.16 (m, 4H), 7.09 (t, J = 7.4 Hz, 2H). MS (mass m/z): calcd for $C_{36}H_{21}NS_2H^+$ $[M+H]^+$ 532.1188, found $C_{36}H_{21}NS_2H^+$ $[M+H]^+$ 532.1189.

Synthesis of PTBT-O-NPh_2: Sodium Bicarbonate (1.06 g, 12.6 mmol) was added to the flask which contains compound PTBT-NPh_2 (60 mg, 0.11 mmol) in the solution of (Acetone/DCM/H2O=1:1:1, 9 mL) and then, it was cooled down to -10 ℃. Then oxone (1.09 g, 7.2 mmol) was added to the solution slowly. The mixture was stirred at -10 ℃ for 2 h. Then 10 mL of $Na_2S_2O_3$ solution was added to the solution and the organic layer was separated. The aqueous layer was extracted two times with 20 mL of dichloromethane. And then, combined extracts were dried over Na_2SO_4. The solvent was evaporated and the residue was purified by silica gel column chromatography using dichloromethane/hexane=1:20 as eluent to obtain purple powder of PTBT-O-NPh_2. Yield: 5.6 mg (8.3 %) MS (mass m/z): calcd for $C_{36}H_{21}NO_4S_2Na^+$ $[M+Na]^+$ 618.0804, found for $C_{36}H_{21}NO_4S_2Na^+$ $[M+Na]^+$ 618.0905.

3. Characterization spectroscopy

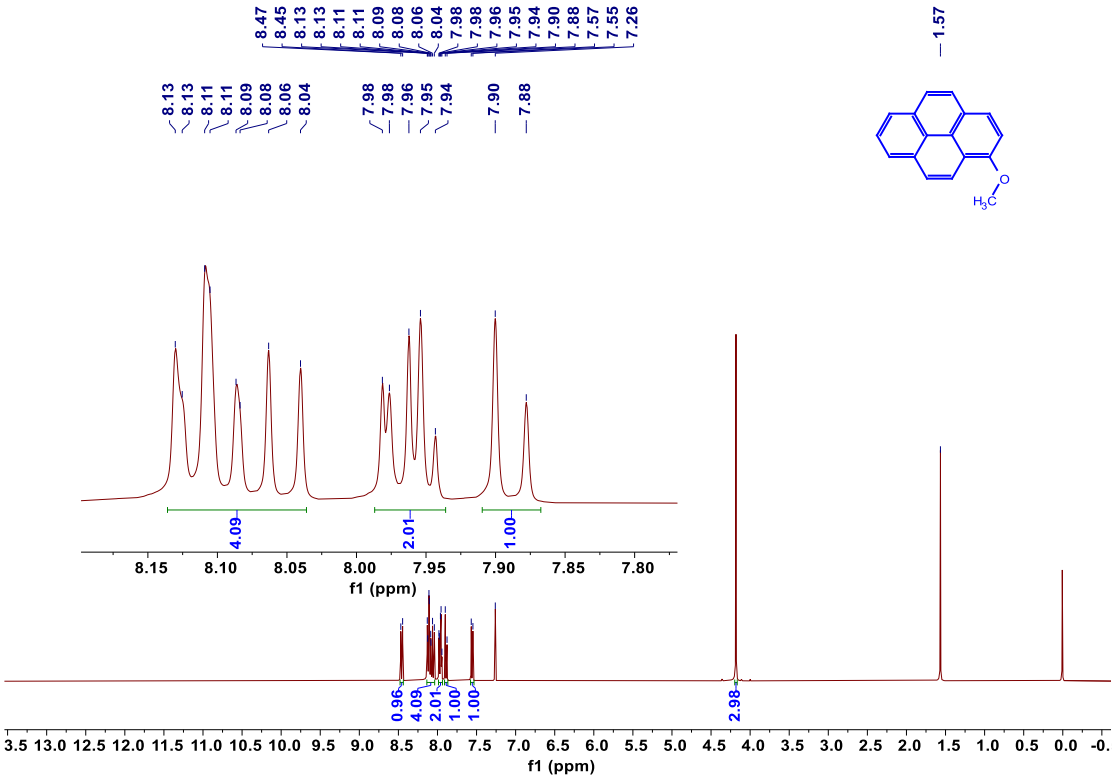

Figure S1 ^{1}H NMR spectrum of **S-1**

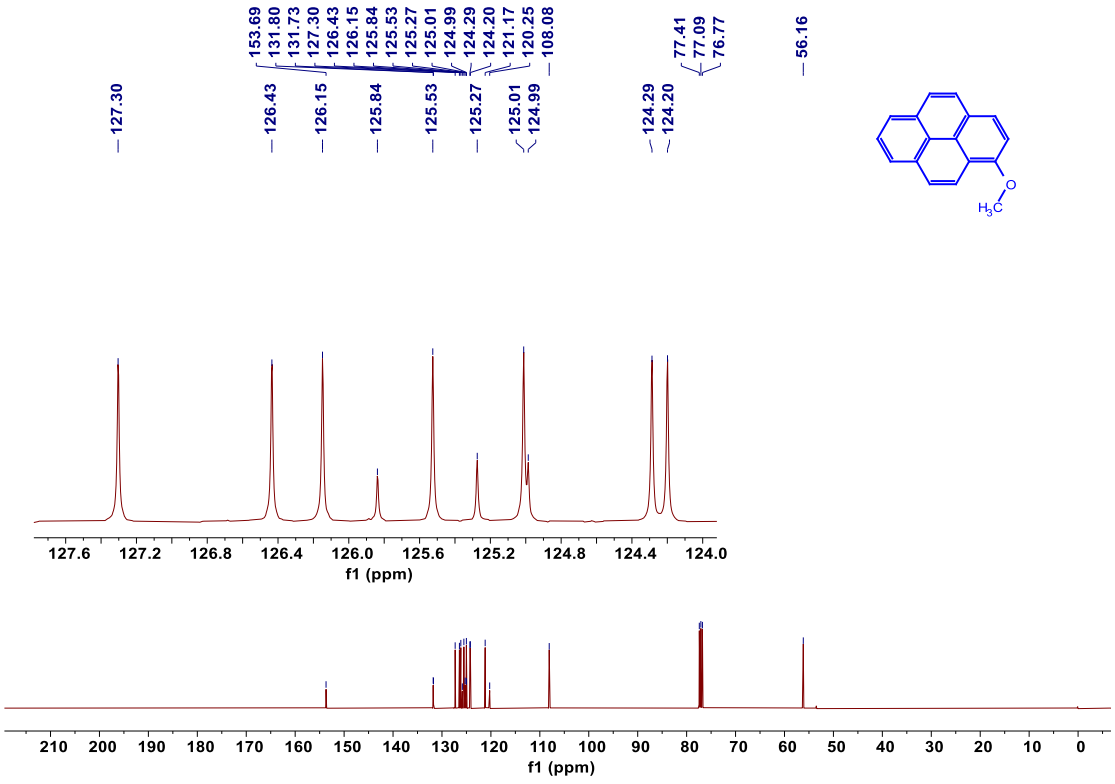

Figure S2 ^{13}C NMR spectrum of **S-1**

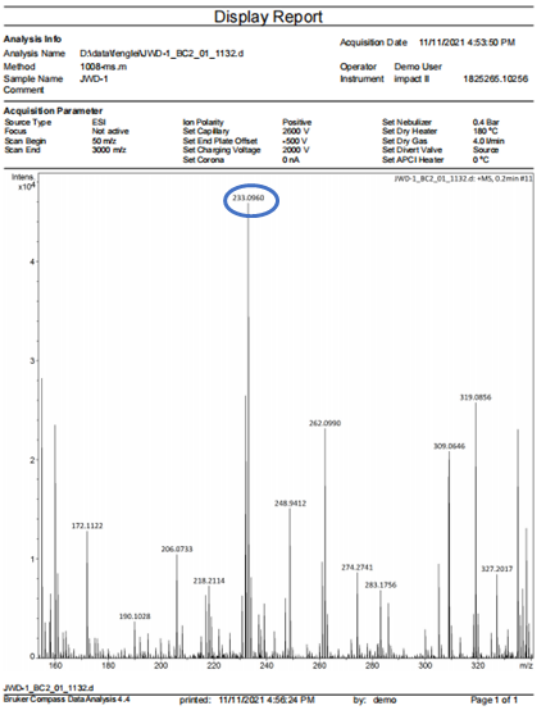

Figure S3 HRMS spectra of **S-1**

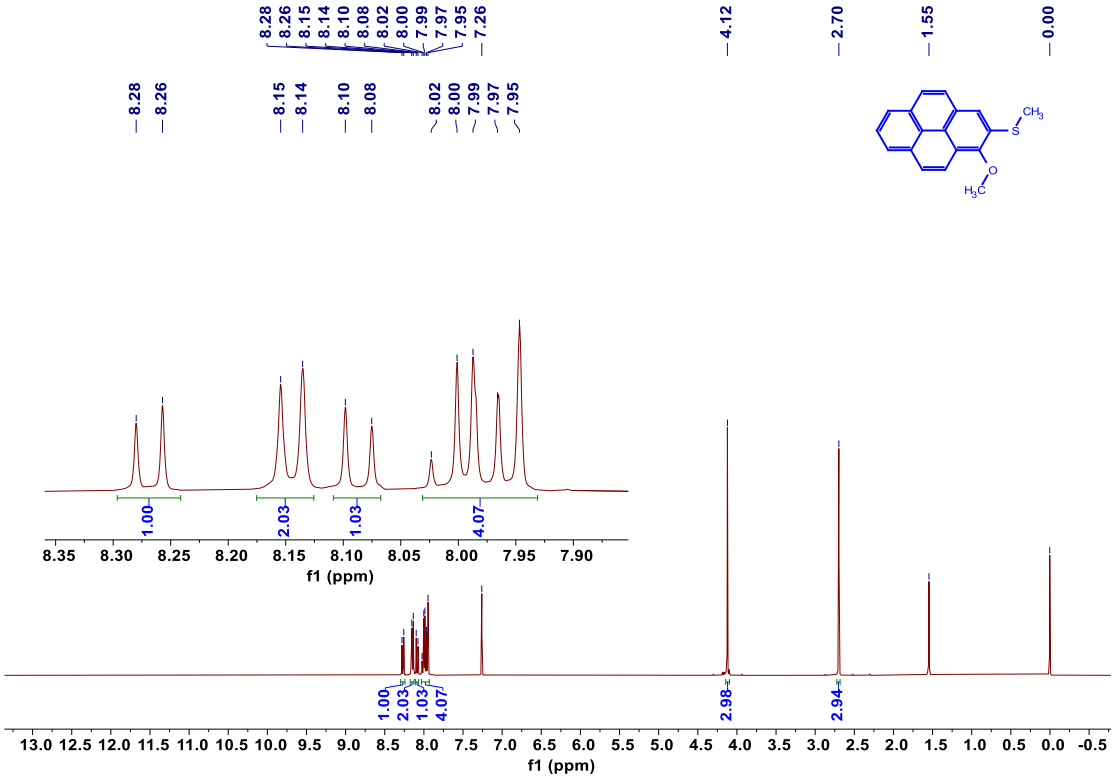

Figure S4 ^{1}H NMR spectrum of **S-2**

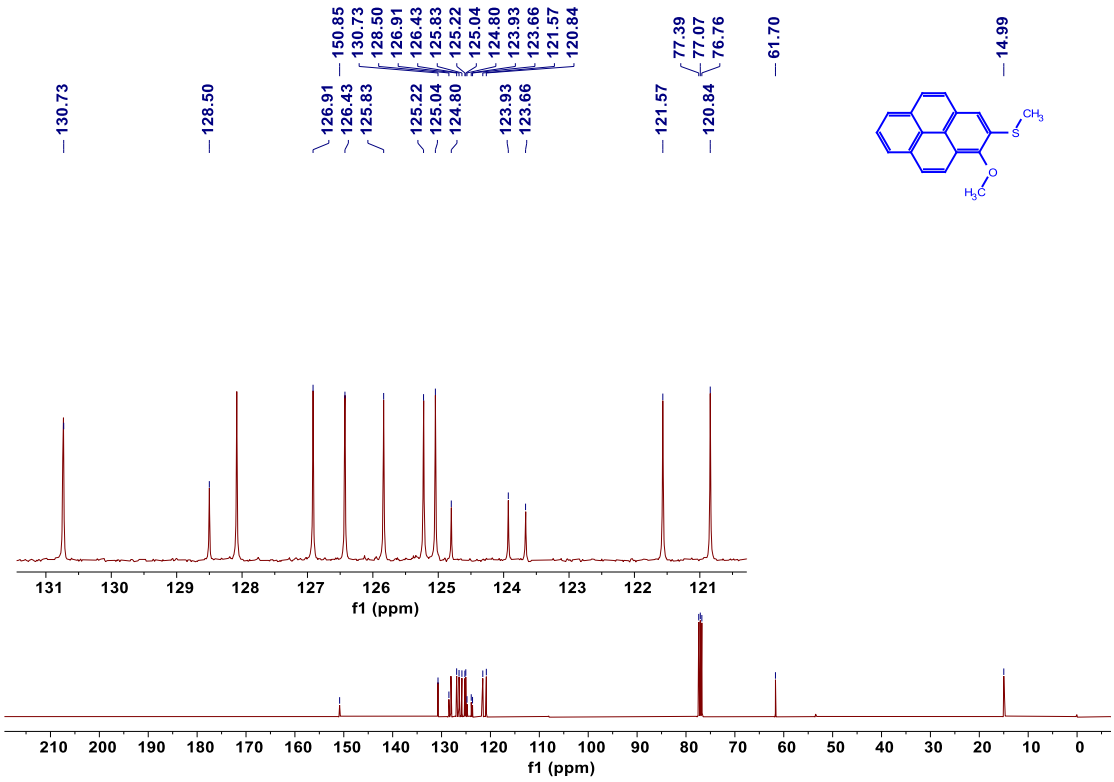

Figure S5 ^{13}C NMR spectrum of **S-2**

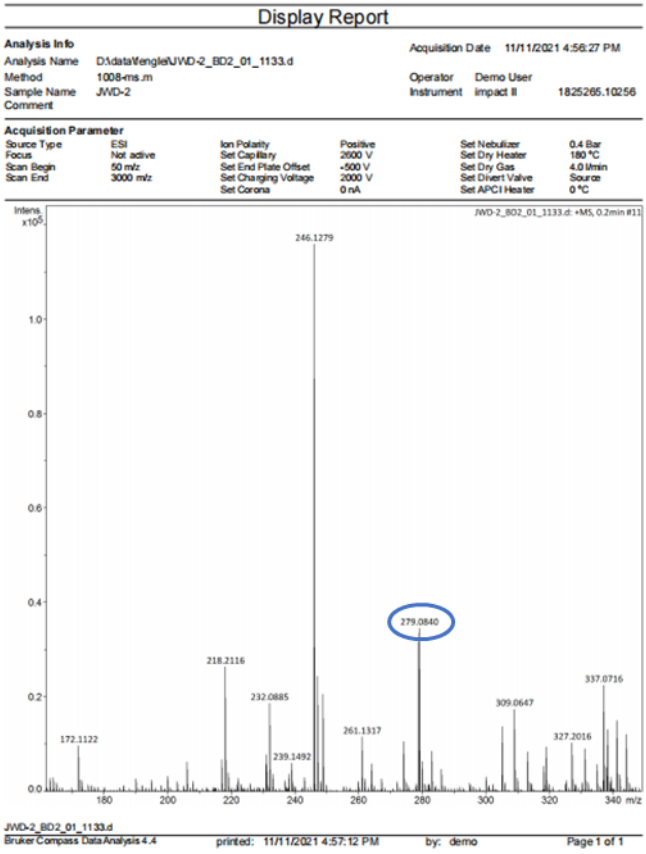

Figure S6 HRMS spectra of **S-2**

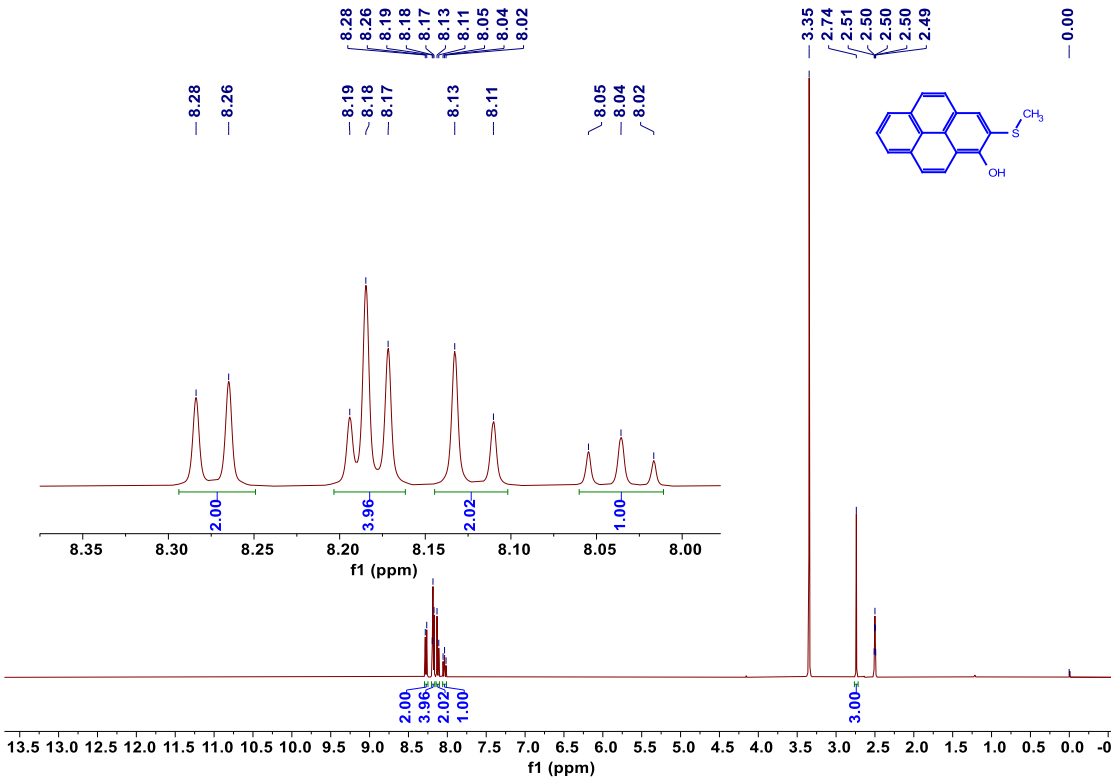

Figure S7 ^{1}H NMR spectrum of **S-3**

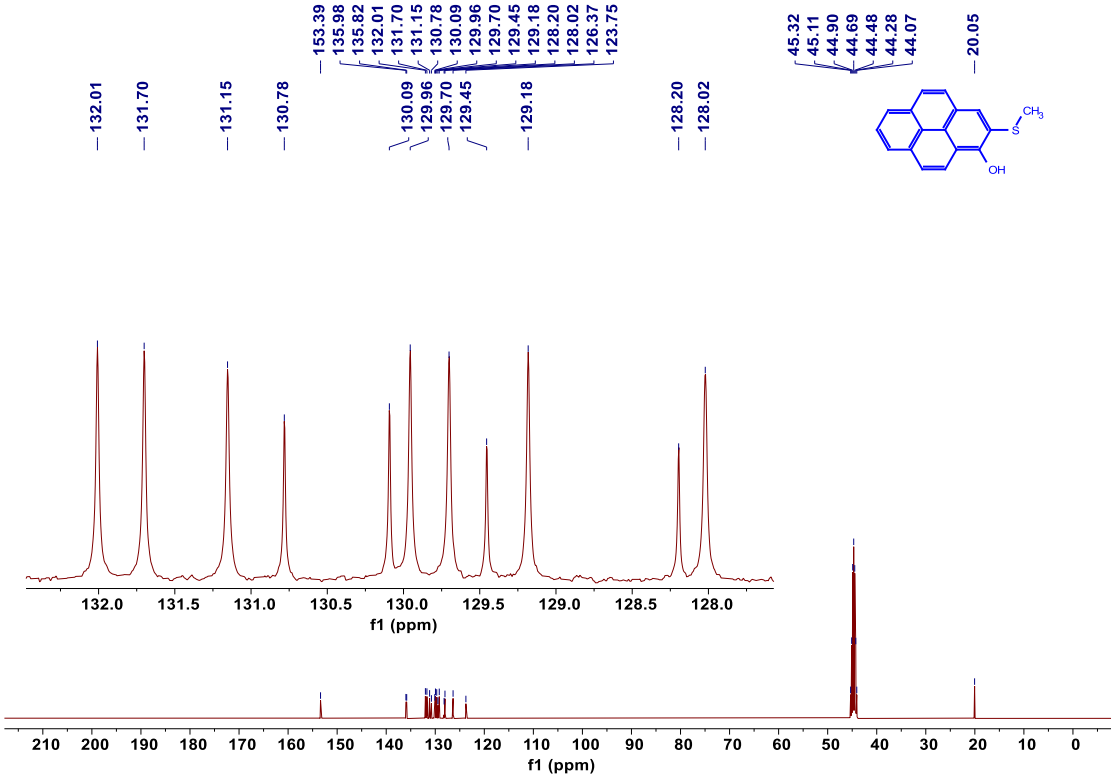

Figure S8 ^{13}C NMR spectrum of **S-3**

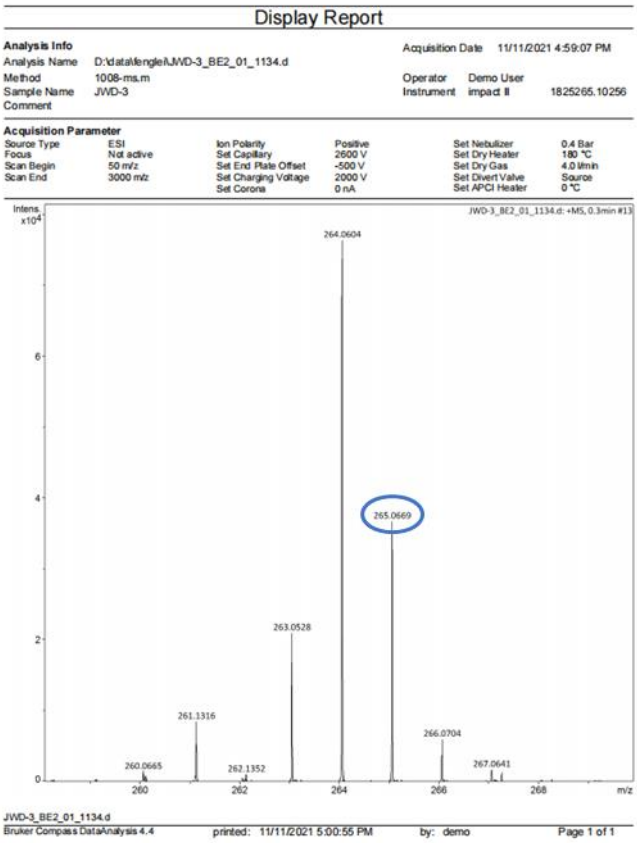

Figure S9 HRMS spectra of **S-3**

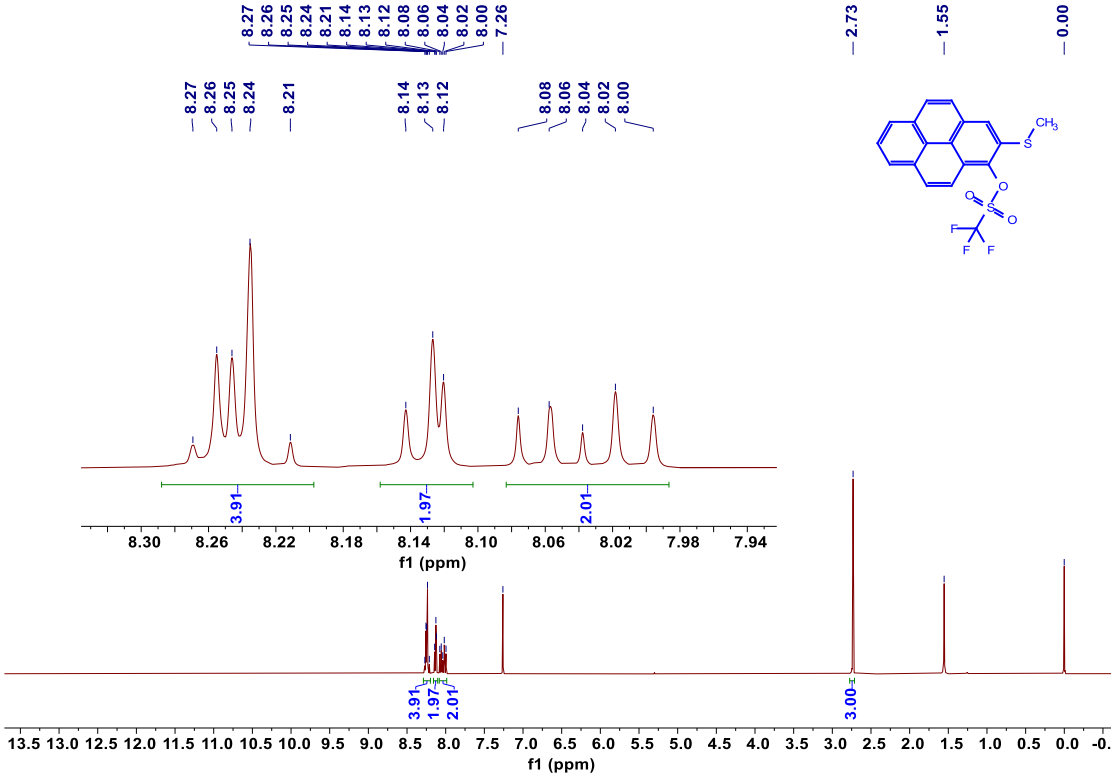

Figure S10 ^{1}H NMR spectrum of **S-4**

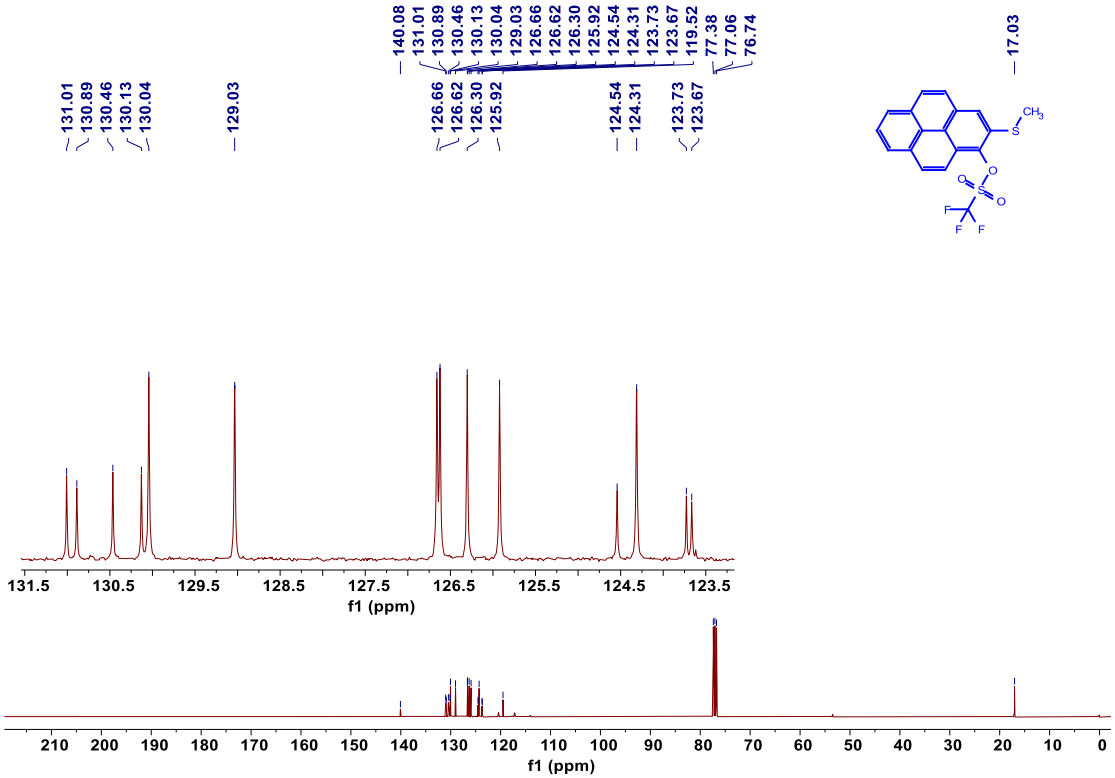

Figure S11 ^{13}C NMR spectrum of **S-4**

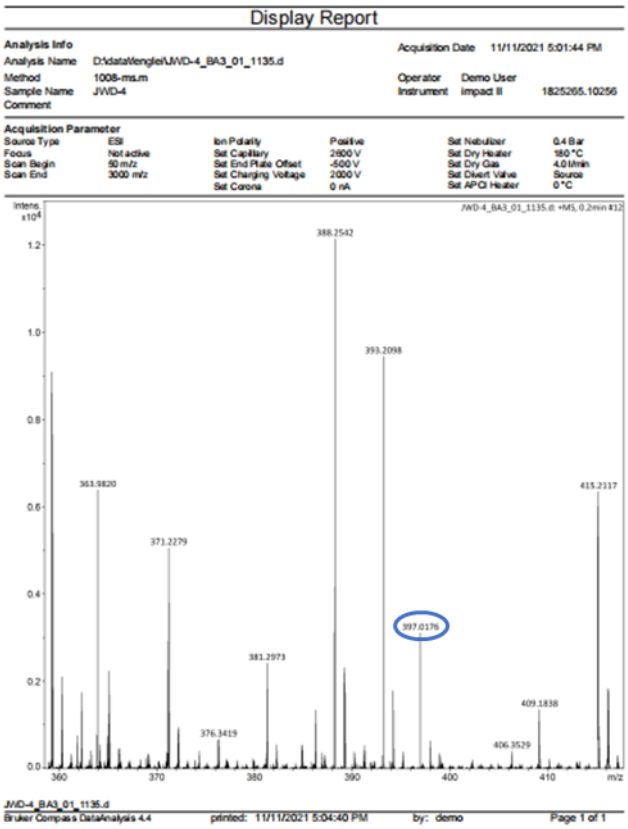

Figure S12 HRMS spectra of S-4

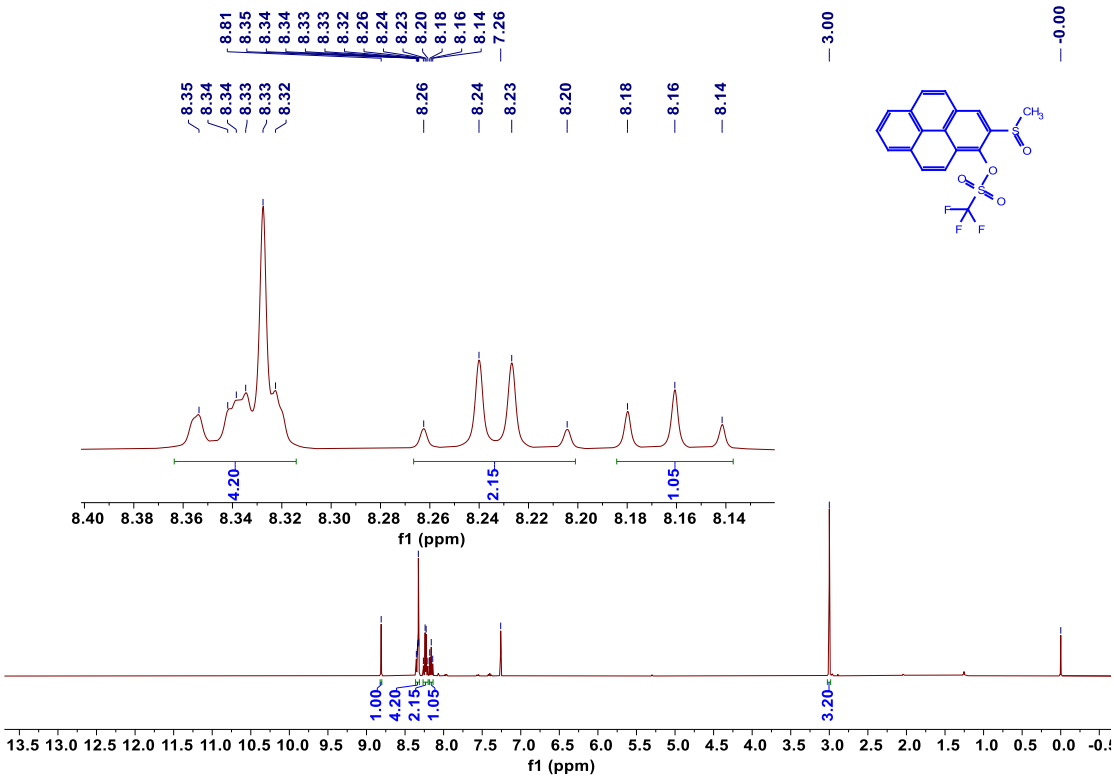

Figure S13 ^{1}H NMR spectrum of S-5

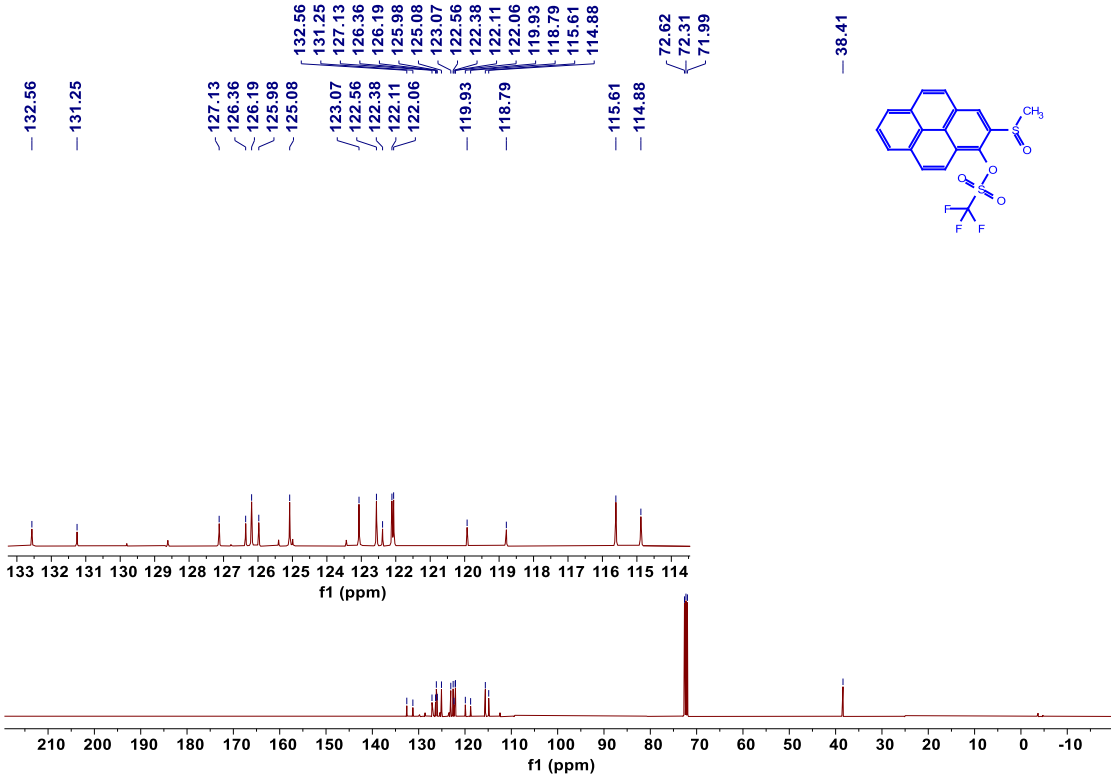

Figure S14 ^{13}C NMR spectrum of **S-5**

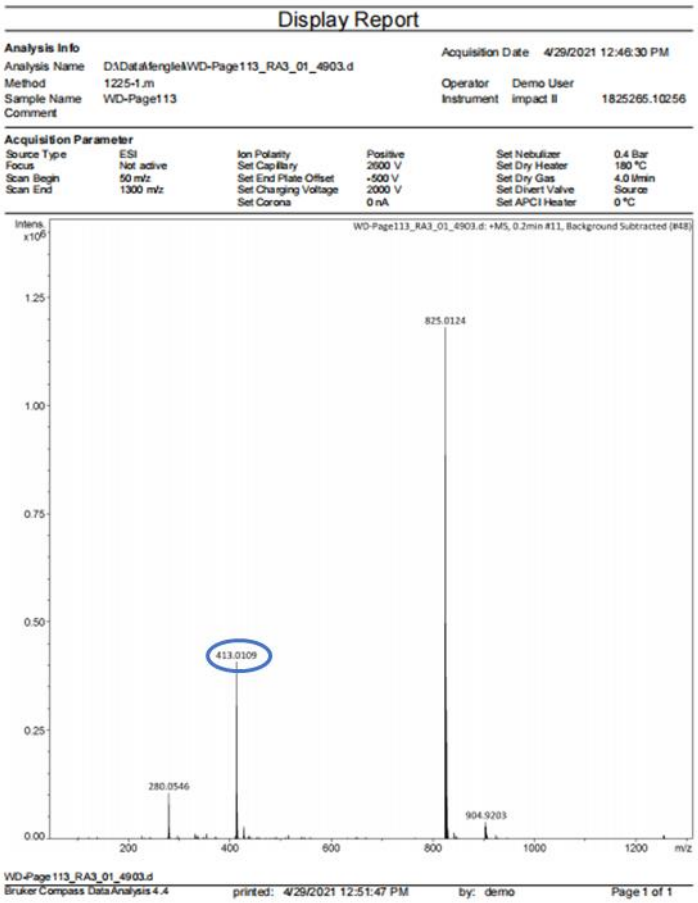

Figure S15 HRMS spectra of **S-5**

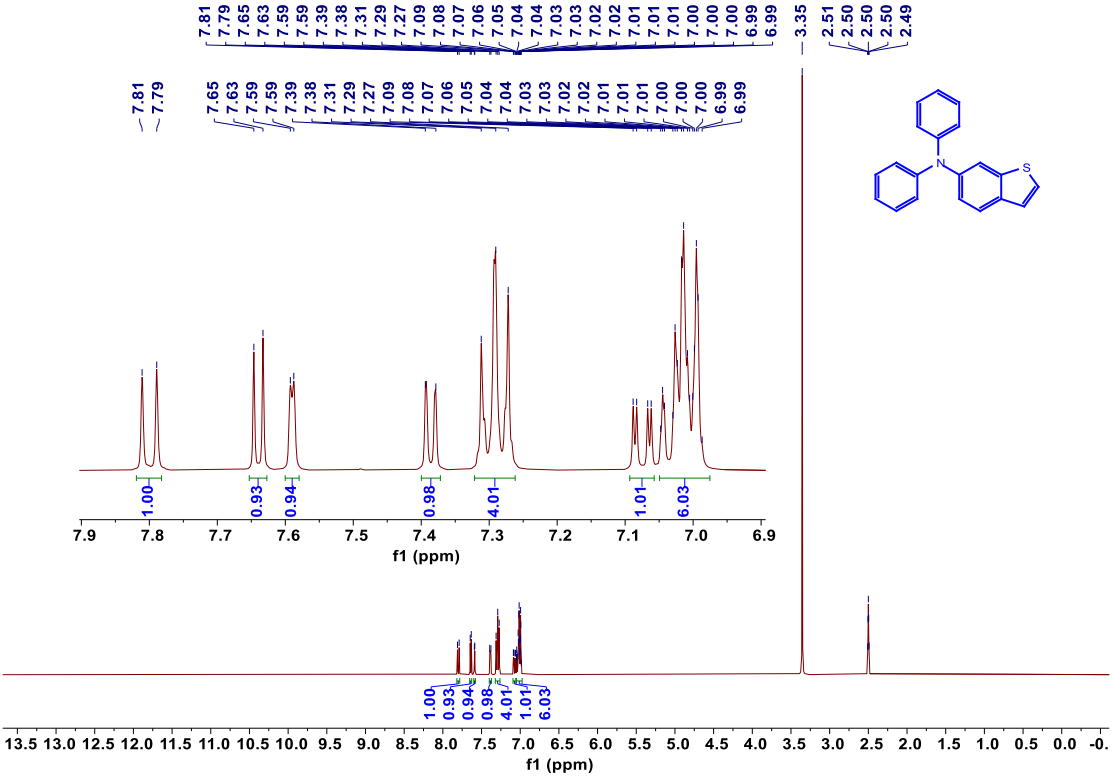

Figure S16 ^{1}H NMR spectrum of **S-6**

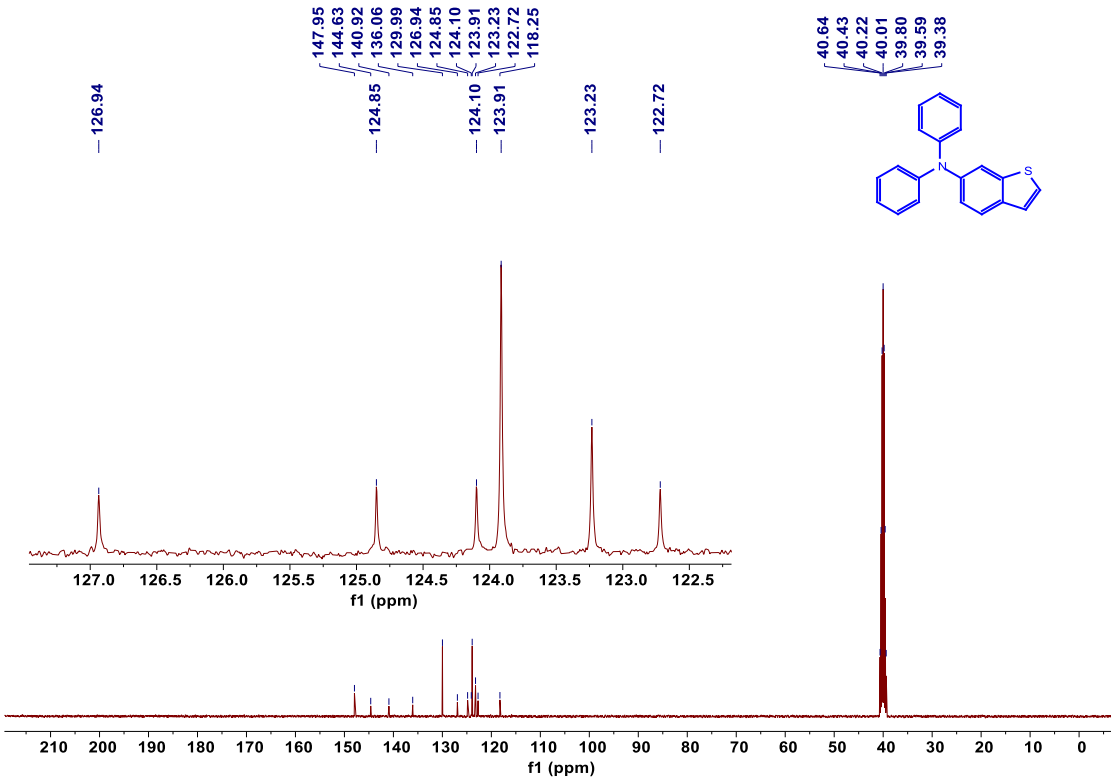

Figure S17 ^{13}C NMR spectrum of **S-6**

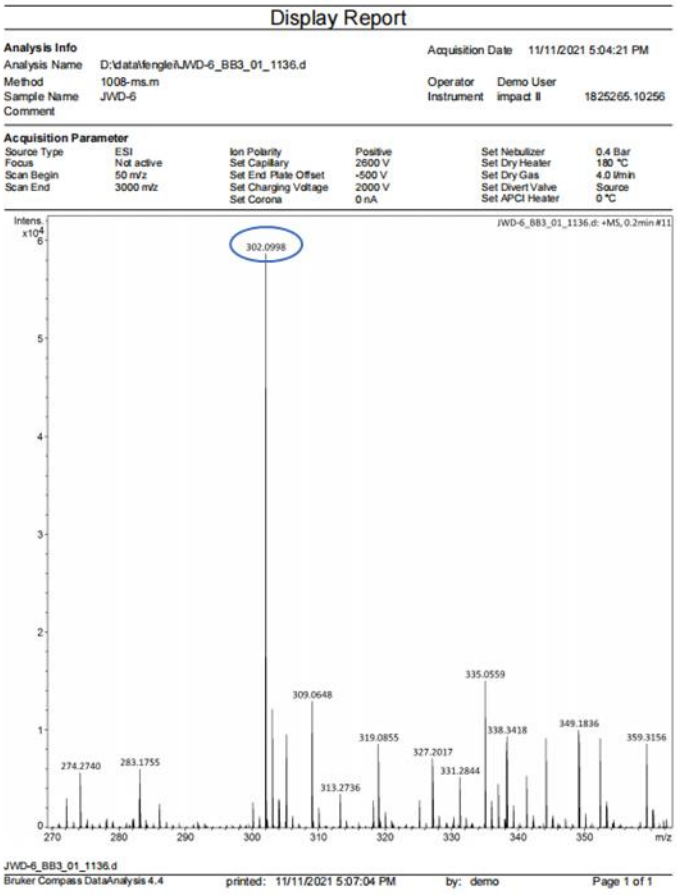

Figure S18 HRMS spectra of **S-6**

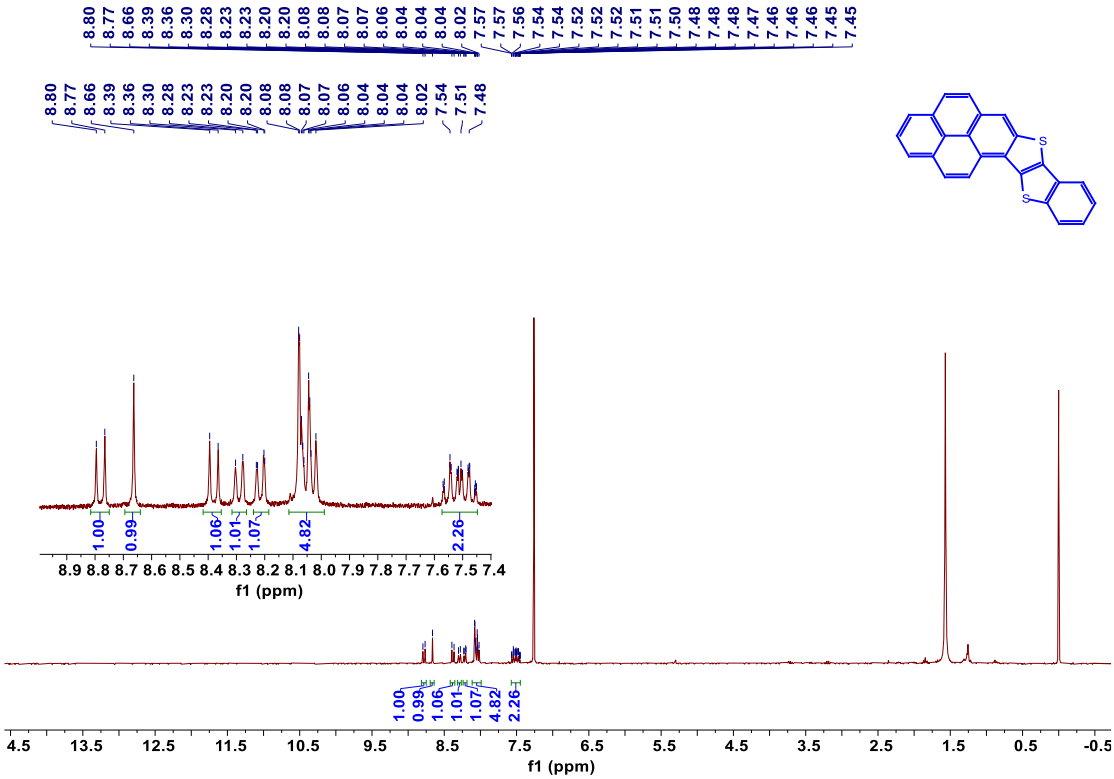

Figure S19 ^{1}H NMR spectrum of **PTBT-H**

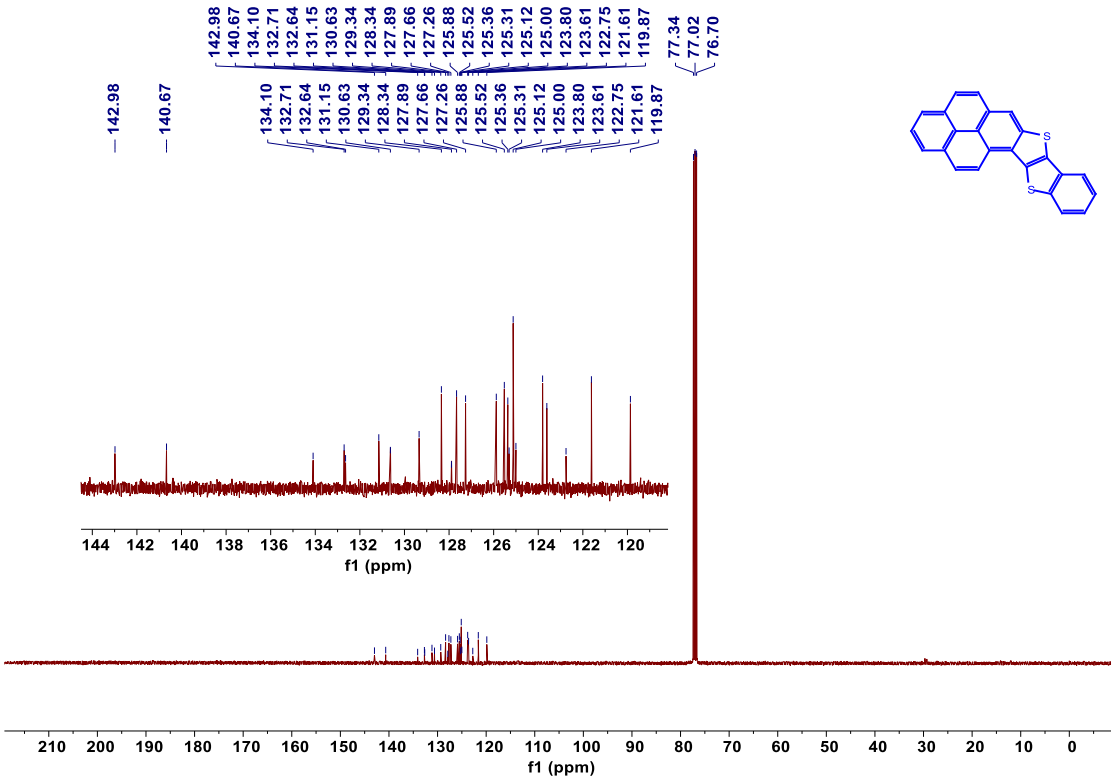

Figure S20 ^{13}C NMR spectrum of **PTBT-H**

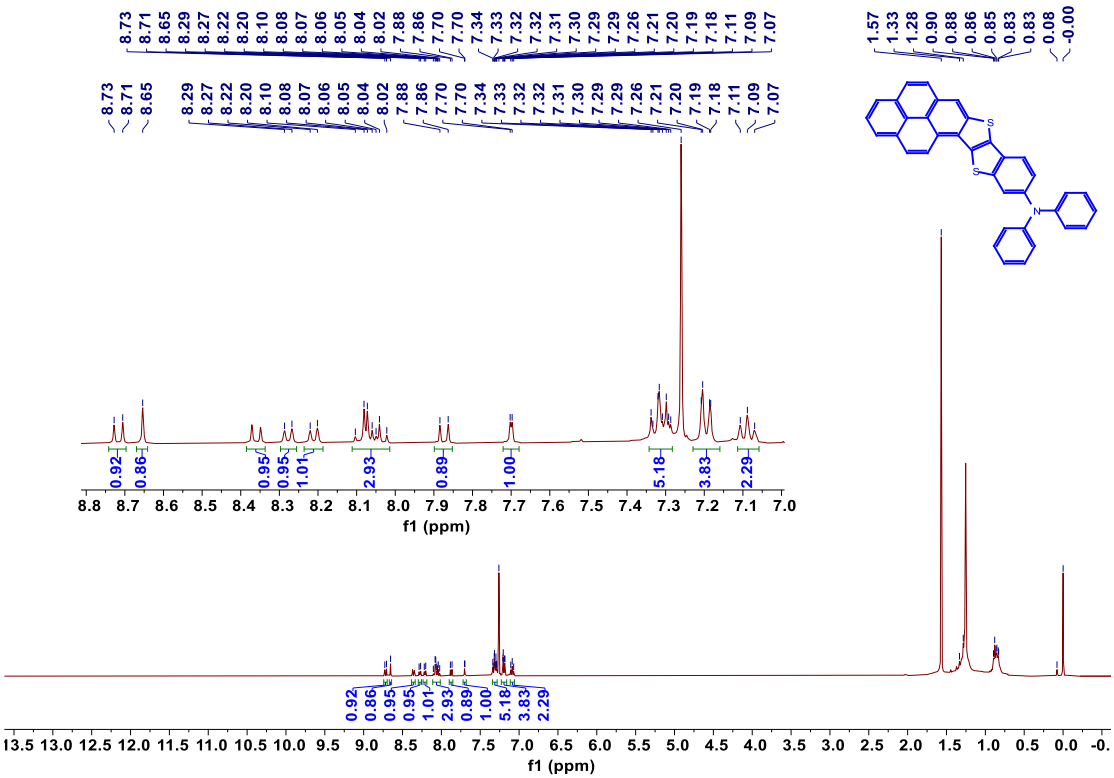

Figure S21 ^{1}H NMR spectrum of **PTBT-NPh$_2$**

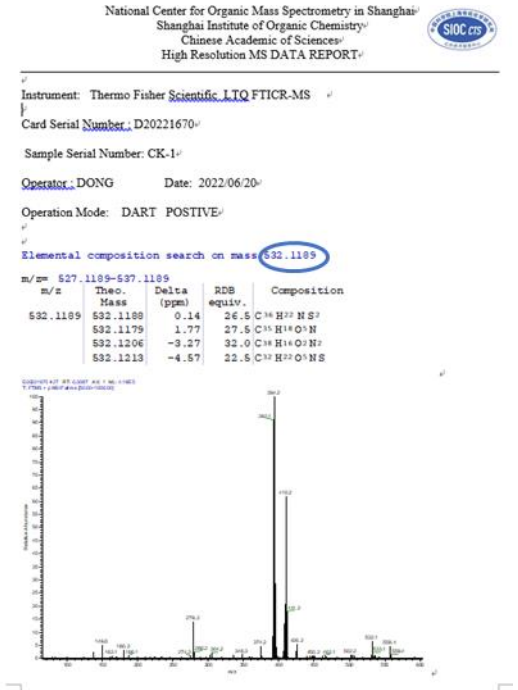

National Center for Organic Mass Spectrometry in Shanghai
Shanghai Institute of Organic Chemistry
Chinese Academic of Sciences
High Resolution MS DATA REPORT

Instrument: Thermo Fisher Scientific LTQ FTICR-MS

Card Serial Number : D20221670

Sample Serial Number: CK-1

Operator : DONG Date: 2022/06/20

Operation Mode: DART POSTIVE

Elemental composition search on mass 532.1189

m/z= 527.1189-537.1189

m/z	Theo. Mass	Delta (ppm)	RDB equiv.	Composition
532.1189	532.1188	0.14	26.5	$C_{36}H_{22}NS_2$
	532.1179	1.77	27.5	$C_{35}H_{14}O_3N$
	532.1206	-3.27	32.0	$C_{38}H_{14}O_2N_2$
	532.1213	-4.57	22.5	$C_{32}H_{22}O_3NS$

Figure S22 HRMS spectra of **PTBT-NPh$_2$**

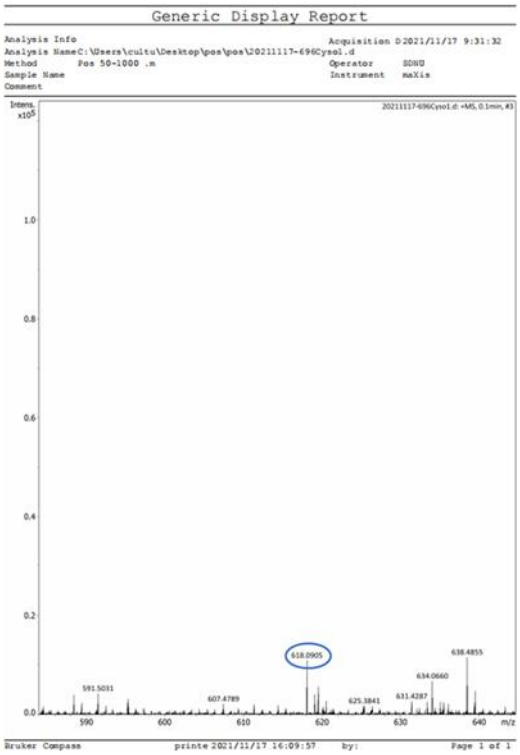

Figure S23 HRMS spectra of **PTBT-O-NPh$_2$**

4. X-Ray Crystal Structure Determination

Table S2 Crystal data and structure refinement for **PTBT-H**, **PTBT-NPh$_2$** and **PTBT-O-NPh$_2$**

Identification code	**PTBT-H**	**PTBT-NPh$_2$**	**PTBT-O-NPh$_2$**
Empirical formula	$C_{24}H_{12}S_2$	$C_{36}H_{21}NS_2$	$C_{36}H_{21}NO_4S_2$
Formula weight	364.46	531.66	595.66
Temperature/K	296.0	173.00(2)	173.00(2)
Crystal system	orthorhombic	triclinic	triclinic
Space group	$Pca2_1$	P-1	P-1
a/Å	24.0909(15)	10.9728(4)	12.0120(3)
b/Å	3.9416(3)	12.1051(3)	14.3623(4)
c/Å	33.935(2)	20.2333(7)	16.3253(3)
α/°	90	85.395(2)	94.8658(19)
β/°	90	77.868(3)	93.9589(18)
γ/°	90	79.709(2)	103.292(3)
Volume/Å^3	3222.3(4)	2582.68(14)	2719.71(13)
Z	4	4	4
ρ_{calc}g/cm^3	1.503	1.367	1.455
μ/mm^{-1}	3.005	2.07	2.144
F(000)	1504.0	1104	1232
Radiation	CuKα (λ = 1.54178)	Cu Kα (λ = 1.54184)	Cu Kα (λ = 1.54184)
2Θ range for data collection/°	7.338 to 133.22	7.43 to 134.126	6.358 to 134.16
Index ranges	-28 ≤ h ≤ 27, -4 ≤ k ≤ 4, -40 ≤ l ≤ 39	-13 ≤ h ≤ 12, -12 ≤ k ≤ 14, -24 ≤ l ≤ 24	-14 ≤ h ≤ 14, -17 ≤ k ≤ 17, -19 ≤ l ≤ 15
Reflections collected	16236	26827	27574
Independent reflections	5623 [Rint = 0.0661, Rsigma = 0.0730]	9096 [R_{int} = 0.0473, R_{sigma} = 0.0525]	9572 [R_{int} = 0.0664, R_{sigma} = 0.0682]
Data/restraints/parameters	5623/1/469	9096/0/703	9572/72/775
Goodness-of-fit on F^2	0.993	1.05	1.051
Final R indexes [I>=2σ (I)]	R1 = 0.0454, wR2 = 0.0976	R_1 = 0.0362, wR_2 = 0.0921	R_1 = 0.0587, wR_2 = 0.1579
Final R indexes [all data]	R1 = 0.0685, wR2 = 0.1077	R_1 = 0.0472, wR_2 = 0.0968	R_1 = 0.0707, wR_2 = 0.1647
Largest diff. peak/hole / e Å^{-3}	0.21/-0.27	0.26/-0.30	0.45/-0.40

Table S3 Bond Lengths for **PTBT-H**

Atom	Atom	Length/Å	Atom	Atom	Length/Å
S2	C19	1.760(6)	C7	C8	1.406(8)
S2	C2	1.752(6)	C7	C18	1.425(8)
S1	C1	1.723(6)	C8	C9	1.365(9)
S1	C16	1.751(6)	C9	C10	1.382(9)
C23	C24	1.373(9)	C1	C20	1.437(8)
C23	C22	1.380(9)	C16	C15	1.377(8)
C24	C19	1.393(8)	C15	C14	1.389(8)
C19	C20	1.391(8)	C14	C13	1.416(8)
C2	C3	1.433(8)	C14	C17	1.436(8)
C2	C1	1.375(8)	C13	C12	1.352(9)
C3	C4	1.403(8)	C12	C11	1.441(8)
C3	C16	1.416(7)	C11	C18	1.406(8)
C4	C5	1.444(7)	C11	C10	1.400(8)
C4	C17	1.415(8)	C18	C17	1.427(8)
C5	C6	1.346(8)	C20	C21	1.398(8)
C6	C7	1.416(8)	C21	C22	1.369(9)

Table S4 Bond Angles for **PTBT-H**

Atom	Atom	Atom	Angle/°	Atom	Atom	Atom	Angle/°
C2	S2	C19	90.6(3)	C18	C11	C12	119.7(5)
C1	S1	C16	90.7(3)	C10	C11	C18	119.2(6)
C4	C3	C2	131.7(5)	C10	C11	C12	121.1(6)
C4	C3	C16	118.9(5)	C22	C21	C20	118.1(6)
C16	C3	C2	109.3(5)	C15	C14	C13	122.3(5)
C16	C15	C14	120.6(5)	C15	C14	C17	118.7(5)
C9	C8	C7	121.1(6)	C13	C14	C17	119.0(6)
C12	C13	C14	122.7(6)	C13	C12	C11	119.5(6)
C3	C2	S2	134.2(4)	C24	C19	S2	126.0(5)
C1	C2	S2	111.4(4)	C20	C19	S2	112.9(4)
C1	C2	C3	114.4(5)	C20	C19	C24	121.0(6)
C6	C5	C4	120.8(6)	C2	C1	S1	112.6(4)
C23	C24	C19	118.2(6)	C2	C1	C20	114.6(5)
C4	C17	C18	120.8(5)	C20	C1	S1	132.8(5)
C4	C17	C14	120.6(5)	C24	C23	C22	120.7(6)
C18	C17	C14	118.5(5)	C3	C16	S1	112.9(4)
C3	C4	C5	122.8(5)	C15	C16	S1	125.2(5)
C3	C4	C17	119.3(5)	C15	C16	C3	121.9(6)
C17	C4	C5	117.9(5)	C8	C7	C18	118.1(6)
C11	C18	C17	120.5(5)	C8	C7	C6	123.5(6)
C11	C18	C7	120.1(5)	C6	C7	C18	118.3(5)
C7	C18	C17	119.4(5)	C9	C10	C11	120.4(6)
C21	C20	C1	129.6(6)	C5	C6	C7	122.8(6)
C19	C20	C21	120.0(6)	C8	C9	C10	121.1(6)
C19	C20	C1	110.4(5)				

Table S5 Torsion Angles for **PTBT-H**

A	B	C	D	Angle/°	A	B	C	D	Angle/°
S2	C2	C1	S1	-179.8(3)	C18	C7	C6	C5	-0.3(9)
S2	C2	C1	C20	-0.3(6)	C11	C18	C7	C8	-0.3(8)
S2	C19	C20	C21	179.2(4)	C11	C18	C7	C6	-179.4(5)
S2	C19	C20	C1	-0.8(6)	C11	C10	C9	C8	1.3(10)
S1	C1	C20	C21	0.1(10)	C14	C15	C16	S1	178.7(5)
S1	C1	C20	C19	-179.9(5)	C14	C15	C16	C3	-0.6(9)
C3	C2	C1	S1	0.7(6)	C14	C13	C12	C11	0.7(9)
C3	C2	C1	C20	-179.8(5)	C14	C17	C4	C3	0.1(8)
C8	C7	C6	C5	-179.4(6)	C14	C17	C4	C5	179.3(5)
C2	S2	C19	C24	179.6(5)	C14	C17	C18	C11	0.1(8)
C2	S2	C19	C20	0.6(5)	C14	C17	C18	C7	-179.4(5)
C2	C3	C4	C5	1.2(10)	C12	C13	C14	C15	-179.0(6)
C2	C3	C4	C17	-179.7(6)	C12	C13	C14	C17	0.3(9)
C2	C3	C16	S1	0.5(6)	C12	C11	C10	C9	179.2(6)
C2	C3	C16	C15	179.8(5)	C19	S2	C2	C3	179.2(6)
C2	C1	C20	C21	-179.3(6)	C19	S2	C2	C1	-0.2(4)
C2	C1	C20	C19	0.7(7)	C19	C24	C23	C22	1.4(9)
C24	C19	C20	C21	0.1(9)	C1	S1	C16	C3	-0.1(5)
C24	C19	C20	C1	-179.9(5)	C1	S1	C16	C15	-179.4(6)
C24	C23	C22	C21	-0.9(10)	C23	C24	C19	S2	-180.0(5)
C17	C18	C11	C12	0.9(8)	C23	C24	C19	C20	-1.0(9)
C17	C18	C11	C10	-179.5(5)	C16	S1	C1	C2	-0.3(4)
C17	C18	C7	C8	179.2(6)	C16	S1	C1	C20	-179.7(6)
C17	C18	C7	C6	0.1(8)	C16	C3	C2	S2	179.9(5)
C4	C3	C2	S2	0.1(10)	C16	C3	C2	C1	-0.8(7)
C4	C3	C2	C1	179.5(6)	C16	C3	C4	C5	-178.6(5)
C4	C3	C16	S1	-179.7(4)	C16	C3	C4	C17	0.6(8)
C4	C3	C16	C15	-0.3(8)	C16	C15	C14	C13	-179.5(6)
C4	C5	C6	C7	0.3(10)	C16	C15	C14	C17	1.2(9)
C4	C17	C18	C11	179.7(5)	C22	C21	C20	C19	0.4(9)
C4	C17	C18	C7	0.2(8)	C22	C21	C20	C1	-179.5(6)
C4	C17	C14	C15	-1.0(8)	C7	C8	C9	C10	-1.5(10)
C4	C17	C14	C13	179.7(5)	C7	C18	C11	C12	-179.6(5)
C18	C17	C4	C3	-179.5(5)	C7	C18	C11	C10	0.0(8)
C18	C17	C4	C5	-0.3(8)	C10	C11	C12	C13	179.1(6)
C18	C17	C14	C15	178.6(5)	C6	C5	C4	C3	179.2(6)
C18	C17	C14	C13	-0.7(8)	C6	C5	C4	C17	0.0(8)
C18	C11	C12	C13	-1.3(9)	C9	C8	C7	C18	1.0(9)
C18	C11	C10	C9	-0.5(9)	C9	C8	C7	C6	-179.9(6)
C20	C21	C22	C23	0.0(9)					

Table S6 Bond Lengths for **PTBT-NPh$_2$**

Atom	Atom	Length/Å	Atom	Atom	Length/Å
S4	C38	1.7375(16)	C65	C64	1.378(4)
S4	C55	1.7533(17)	C3	C4	1.414(2)
S3	C37	1.7278(17)	C3	C16	1.416(2)
S3	C52	1.7477(17)	C23	C24	1.389(3)
S1	C1	1.7396(16)	C23	C22	1.403(3)
S1	C16	1.7522(17)	C38	C39	1.432(2)
S2	C2	1.7472(15)	C67	C68	1.381(3)
S2	C19	1.7480(17)	C67	C72	1.382(3)
N2	C67	1.431(2)	C52	C39	1.414(2)
N2	C61	1.415(2)	C55	C60	1.395(2)
N2	C59	1.420(2)	C55	C56	1.404(2)
N1	C23	1.431(2)	C41	C40	1.424(2)
N1	C25	1.406(2)	C62	C61	1.389(3)
N1	C31	1.424(2)	C15	C14	1.391(2)
C51	C50	1.388(3)	C15	C16	1.390(2)
C51	C52	1.392(2)	C39	C40	1.418(2)
C63	C62	1.381(3)	C6	C5	1.353(3)
C63	C64	1.368(4)	C6	C7	1.433(2)
C71	C70	1.376(3)	C13	C14	1.438(2)
C71	C72	1.380(3)	C13	C12	1.348(3)
C54	C53	1.427(2)	C18	C7	1.423(2)
C54	C43	1.414(2)	C18	C17	1.428(2)
C54	C47	1.426(2)	C25	C26	1.398(2)
C10	C11	1.395(3)	C25	C30	1.400(2)
C10	C9	1.388(3)	C32	C31	1.386(3)
C37	C38	1.374(2)	C19	C20	1.416(2)
C37	C56	1.429(2)	C19	C24	1.391(2)
C42	C41	1.356(2)	C35	C36	1.388(3)
C42	C43	1.437(2)	C35	C34	1.377(3)
C53	C50	1.433(2)	C57	C56	1.403(2)
C53	C40	1.427(2)	C36	C31	1.392(3)
C48	C49	1.351(3)	C20	C21	1.400(2)
C48	C47	1.435(3)	C20	C1	1.431(2)
C11	C18	1.428(2)	C60	C59	1.390(2)
C11	C12	1.439(3)	C14	C17	1.428(2)
C2	C3	1.435(2)	C9	C8	1.382(3)
C2	C1	1.365(2)	C21	C22	1.378(2)
C45	C44	1.384(3)	C44	C43	1.406(2)
C45	C46	1.381(3)	C61	C66	1.389(3)
C27	C26	1.384(3)	C8	C7	1.403(3)
C27	C28	1.385(3)	C46	C47	1.396(3)
C50	C49	1.442(2)	C5	C4	1.430(2)

C33	C32	1.394(3)	C68	C69	1.390(3)
C33	C34	1.380(3)	C30	C29	1.386(3)
C58	C57	1.371(3)	C4	C17	1.425(2)
C58	C59	1.408(3)	C70	C69	1.372(3)
C65	C66	1.397(3)	C29	C28	1.381(3)

Table S7 Bond Angles for **PTBT-NPh$_2$**

Atom	Atom	Atom	Angle/°	Atom	Atom	Atom	Angle/°
C38	S4	C55	91.04(8)	C30	C25	N1	121.15(15)
C37	S3	C52	90.53(8)	C31	C32	C33	119.69(17)
C1	S1	C16	90.19(8)	C20	C19	S2	112.59(12)
C2	S2	C19	90.81(8)	C24	C19	S2	125.58(13)
C61	N2	C67	118.21(14)	C24	C19	C20	121.83(15)
C61	N2	C59	121.08(15)	C34	C35	C36	120.33(18)
C59	N2	C67	118.56(14)	C58	C57	C56	119.60(16)
C25	N1	C23	119.51(14)	C35	C36	C31	119.97(18)
C25	N1	C31	120.53(13)	C41	C40	C53	118.64(14)
C31	N1	C23	119.96(14)	C39	C40	C53	118.11(14)
C50	C51	C52	119.33(16)	C39	C40	C41	123.25(15)
C64	C63	C62	120.9(2)	C19	C20	C1	109.79(15)
C70	C71	C72	120.52(19)	C21	C20	C19	118.77(15)
C43	C54	C53	120.47(15)	C21	C20	C1	131.44(15)
C43	C54	C47	119.44(15)	C59	C60	C55	118.15(16)
C47	C54	C53	120.09(16)	C15	C14	C13	121.22(15)
C9	C10	C11	121.06(17)	C15	C14	C17	120.00(14)
C38	C37	S3	112.84(12)	C17	C14	C13	118.77(15)
C38	C37	C56	114.56(15)	C27	C26	C25	120.73(16)
C56	C37	S3	132.58(13)	C8	C9	C10	120.49(18)
C41	C42	C43	121.01(16)	C23	C24	C19	118.08(15)
C54	C53	C50	119.76(15)	C22	C21	C20	119.46(16)
C54	C53	C40	119.51(15)	C45	C44	C43	120.31(17)
C40	C53	C50	120.74(15)	C62	C61	N2	121.78(17)
C49	C48	C47	121.70(16)	C66	C61	N2	119.27(18)
C10	C11	C18	119.11(17)	C66	C61	C62	118.95(17)
C10	C11	C12	122.67(16)	C55	C56	C37	110.39(15)
C18	C11	C12	118.21(16)	C57	C56	C37	131.10(16)
C3	C2	S2	133.90(13)	C57	C56	C55	118.50(15)
C1	C2	S2	111.79(12)	C9	C8	C7	120.73(17)
C1	C2	C3	114.27(14)	C45	C46	C47	121.34(16)
C46	C45	C44	120.47(16)	C61	C66	C65	119.6(2)
C26	C27	C28	120.38(16)	C6	C5	C4	121.52(15)
C51	C50	C53	120.02(15)	C67	C68	C69	120.42(19)
C51	C50	C49	121.42(16)	C18	C7	C6	118.22(16)

C53	C50	C49	118.56(15)	C8	C7	C6	122.46(16)
C34	C33	C32	120.43(18)	C8	C7	C18	119.31(16)
C57	C58	C59	121.50(16)	C2	C1	S1	112.88(12)
C64	C65	C66	120.7(2)	C2	C1	C20	114.97(14)
C4	C3	C2	131.02(15)	C20	C1	S1	132.14(13)
C4	C3	C16	119.34(14)	C29	C30	C25	119.97(16)
C16	C3	C2	109.61(14)	C3	C4	C5	123.09(14)
C24	C23	N1	119.44(15)	C3	C4	C17	118.32(15)
C24	C23	C22	120.71(15)	C17	C4	C5	118.59(15)
C22	C23	N1	119.86(16)	C54	C43	C42	118.57(15)
C37	C38	S4	111.68(12)	C44	C43	C54	119.60(16)
C37	C38	C39	113.94(15)	C44	C43	C42	121.82(16)
C39	C38	S4	134.38(13)	C32	C31	N1	120.39(16)
C68	C67	N2	120.65(17)	C32	C31	C36	119.65(16)
C68	C67	C72	119.26(18)	C36	C31	N1	119.93(16)
C72	C67	N2	120.07(17)	C3	C16	S1	113.00(12)
C51	C52	S3	124.80(13)	C15	C16	S1	124.65(13)
C51	C52	C39	122.28(15)	C15	C16	C3	122.32(15)
C39	C52	S3	112.91(12)	C21	C22	C23	121.15(16)
C60	C55	S4	125.47(13)	C54	C47	C48	118.63(16)
C60	C55	C56	122.22(15)	C46	C47	C54	118.84(17)
C56	C55	S4	112.30(12)	C46	C47	C48	122.53(16)
C42	C41	C40	121.80(15)	C69	C70	C71	119.85(19)
C63	C62	C61	120.4(2)	C18	C17	C14	119.49(14)
C16	C15	C14	119.20(15)	C4	C17	C18	119.73(15)
C48	C49	C50	121.27(17)	C4	C17	C14	120.77(15)
C52	C39	C38	109.76(14)	C35	C34	C33	119.86(17)
C52	C39	C40	119.52(14)	C28	C29	C30	121.15(16)
C40	C39	C38	130.71(15)	C63	C64	C65	119.3(2)
C5	C6	C7	121.62(16)	C29	C28	C27	119.24(16)
C12	C13	C14	121.49(16)	C71	C72	C67	120.07(19)
C7	C18	C11	119.30(16)	C13	C12	C11	121.63(15)
C7	C18	C17	120.30(15)	C70	C69	C68	119.8(2)
C17	C18	C11	120.41(15)	C58	C59	N2	119.68(16)
C26	C25	N1	120.33(15)	C60	C59	N2	120.39(16)
C26	C25	C30	118.52(15)	C60	C59	C58	119.91(16)

Table S8 Torsion Angles for **PTBT-NPh$_2$**

A	B	C	D	Angle/°	A	B	C	D	Angle/°
S4	C38	C39	C52	-177.00(13)	C49	C48	C47	C46	179.07(17)
S4	C38	C39	C40	4.6(3)	C6	C5	C4	C3	-179.66(16)
S4	C55	C60	C59	-178.61(13)	C6	C5	C4	C17	0.7(2)
S4	C55	C56	C37	-1.13(18)	C13	C14	C17	C18	0.1(2)
S4	C55	C56	C57	177.62(13)	C13	C14	C17	C4	179.02(14)

S3	C37	C38	S4	177.37(8)	C18	C11	C12	C13	0.6(3)
S3	C37	C38	C39	-1.70(18)	C25	N1	C23	C24	-124.86(18)
S3	C37	C56	C55	-176.86(13)	C25	N1	C23	C22	54.7(2)
S3	C37	C56	C57	4.6(3)	C25	N1	C31	C32	-131.30(18)
S3	C52	C39	C38	-1.13(17)	C25	N1	C31	C36	46.8(2)
S3	C52	C39	C40	177.51(12)	C25	C30	C29	C28	-0.5(3)
S2	C2	C3	C4	6.7(3)	C32	C33	C34	C35	1.8(3)
S2	C2	C3	C16	-175.17(13)	C19	S2	C2	C3	179.56(17)
S2	C2	C1	S1	176.62(8)	C19	S2	C2	C1	2.00(13)
S2	C2	C1	C20	-2.44(19)	C19	C20	C21	C22	-0.1(3)
S2	C19	C20	C21	-179.51(13)	C19	C20	C1	S1	-177.25(13)
S2	C19	C20	C1	-0.01(18)	C19	C20	C1	C2	1.6(2)
S2	C19	C24	C23	179.61(13)	C35	C36	C31	N1	-175.81(16)
N2	C67	C68	C69	179.4(2)	C35	C36	C31	C32	2.3(3)
N2	C67	C72	C71	179.94(17)	C57	C58	C59	N2	178.39(18)
N2	C61	C66	C65	-179.56(19)	C57	C58	C59	C60	-3.0(3)
N1	C23	C24	C19	179.38(15)	C36	C35	C34	C33	-2.1(3)
N1	C23	C22	C21	-179.20(16)	C40	C53	C50	C51	-0.4(2)
N1	C25	C26	C27	-178.93(16)	C40	C53	C50	C49	179.83(15)
N1	C25	C30	C29	179.79(16)	C20	C19	C24	C23	-0.1(3)
C51	C50	C49	C48	-178.99(16)	C20	C21	C22	C23	-0.2(3)
C51	C52	C39	C38	-179.90(15)	C60	C55	C56	C37	177.83(15)
C51	C52	C39	C40	-1.3(2)	C60	C55	C56	C57	-3.4(2)
C63	C62	C61	N2	178.7(2)	C14	C15	C16	S1	-176.94(12)
C63	C62	C61	C66	-1.7(3)	C14	C15	C16	C3	1.3(2)
C71	C70	C69	C68	1.5(3)	C14	C13	C12	C11	-0.6(3)
C54	C53	C50	C51	179.15(15)	C26	C27	C28	C29	0.2(3)
C54	C53	C50	C49	-0.6(2)	C26	C25	C30	C29	-0.4(2)
C54	C53	C40	C41	-0.2(2)	C9	C10	C11	C18	0.0(3)
C54	C53	C40	C39	-179.20(13)	C9	C10	C11	C12	179.32(18)
C10	C11	C18	C7	-0.3(2)	C9	C8	C7	C6	179.42(17)
C10	C11	C18	C17	179.05(16)	C9	C8	C7	C18	-0.8(3)
C10	C11	C12	C13	-178.71(18)	C24	C23	C22	C21	0.4(3)
C10	C9	C8	C7	0.6(3)	C24	C19	C20	C21	0.2(2)
C37	S3	C52	C51	178.93(15)	C24	C19	C20	C1	179.74(15)
C37	S3	C52	C39	0.19(12)	C21	C20	C1	S1	2.2(3)
C37	C38	C39	C52	1.80(19)	C21	C20	C1	C2	-179.00(18)
C37	C38	C39	C40	-176.63(15)	C44	C45	C46	C47	-0.4(3)
C42	C41	C40	C53	-0.3(2)	C61	N2	C67	C68	-59.4(2)
C42	C41	C40	C39	178.66(15)	C61	N2	C67	C72	122.01(19)
C53	C54	C43	C42	-0.3(2)	C61	N2	C59	C58	-44.4(3)
C53	C54	C43	C44	178.80(15)	C61	N2	C59	C60	137.02(18)
C53	C54	C47	C48	0.3(2)	C56	C37	C38	S4	-1.44(18)
C53	C54	C47	C46	-178.96(14)	C56	C37	C38	C39	179.48(14)

C53	C50	C49	C48	0.7(3)	C56	C55	C60	C59	2.6(3)
C11	C10	C9	C8	-0.2(3)	C46	C45	C44	C43	0.2(3)
C11	C18	C7	C6	-179.58(15)	C66	C65	C64	C63	-1.8(4)
C11	C18	C7	C8	0.7(2)	C5	C6	C7	C18	-1.7(2)
C11	C18	C17	C14	-0.1(2)	C5	C6	C7	C8	178.06(17)
C11	C18	C17	C4	-178.96(15)	C5	C4	C17	C18	-1.3(2)
C2	S2	C19	C20	-1.11(13)	C5	C4	C17	C14	179.84(14)
C2	S2	C19	C24	179.15(16)	C68	C67	C72	C71	1.3(3)
C2	C3	C4	C5	-0.1(3)	C7	C6	C5	C4	0.8(3)
C2	C3	C4	C17	179.44(15)	C7	C18	C17	C14	179.24(14)
C2	C3	C16	S1	-2.23(17)	C7	C18	C17	C4	0.4(2)
C2	C3	C16	C15	179.33(14)	C1	S1	C16	C3	1.27(12)
C45	C44	C43	C54	0.2(2)	C1	S1	C16	C15	179.67(15)
C45	C44	C43	C42	179.18(15)	C1	C2	C3	C4	-175.81(16)
C45	C46	C47	C54	0.2(2)	C1	C2	C3	C16	2.3(2)
C45	C46	C47	C48	-179.05(16)	C1	C20	C21	C22	-179.44(17)
C50	C51	C52	S3	-177.41(12)	C30	C25	C26	C27	1.3(3)
C50	C51	C52	C39	1.2(2)	C30	C29	C28	C27	0.7(3)
C50	C53	C40	C41	179.35(14)	C4	C3	C16	S1	176.18(12)
C50	C53	C40	C39	0.4(2)	C4	C3	C16	C15	-2.3(2)
C33	C32	C31	N1	175.50(16)	C43	C54	C53	C50	-179.11(14)
C33	C32	C31	C36	-2.6(3)	C43	C54	C53	C40	0.5(2)
C58	C57	C56	C37	179.45(18)	C43	C54	C47	C48	179.48(15)
C58	C57	C56	C55	1.0(3)	C43	C54	C47	C46	0.3(2)
C3	C2	C1	S1	-1.45(19)	C43	C42	C41	C40	0.5(2)
C3	C2	C1	C20	179.48(14)	C31	N1	C23	C24	54.8(2)
C3	C4	C17	C18	179.10(14)	C31	N1	C23	C22	-125.62(18)
C3	C4	C17	C14	0.2(2)	C31	N1	C25	C26	30.1(3)
C23	N1	C25	C26	-150.27(17)	C31	N1	C25	C30	-150.16(17)
C23	N1	C25	C30	29.5(2)	C16	S1	C1	C2	0.11(13)
C23	N1	C31	C32	49.0(2)	C16	S1	C1	C20	178.96(17)
C23	N1	C31	C36	-132.86(18)	C16	C3	C4	C5	-178.16(15)
C38	S4	C55	C60	-178.61(15)	C16	C3	C4	C17	1.4(2)
C38	S4	C55	C56	0.31(13)	C16	C15	C14	C13	-179.79(15)
C38	C37	C56	C55	1.7(2)	C16	C15	C14	C17	0.4(2)
C38	C37	C56	C57	-176.88(17)	C22	C23	C24	C19	-0.2(3)
C38	C39	C40	C53	178.75(15)	C47	C54	C53	C50	0.1(2)
C38	C39	C40	C41	-0.2(3)	C47	C54	C53	C40	179.68(14)
C67	N2	C61	C62	139.43(19)	C47	C54	C43	C42	-179.46(14)
C67	N2	C61	C66	-40.2(3)	C47	C54	C43	C44	-0.4(2)
C67	N2	C59	C58	152.55(17)	C47	C48	C49	C50	-0.4(3)
C67	N2	C59	C60	-26.0(3)	C70	C71	C72	C67	0.8(3)
C67	C68	C69	C70	0.6(3)	C17	C18	C7	C6	1.1(2)
C52	S3	C37	C38	0.85(13)	C17	C18	C7	C8	-178.65(15)

C52	S3	C37	C56	179.39(17)	C34	C33	C32	C31	0.6(3)
C52	C51	C50	C53	-0.4(2)	C34	C35	C36	C31	0.1(3)
C52	C51	C50	C49	179.38(15)	C64	C63	C62	C61	0.8(4)
C52	C39	C40	C53	0.4(2)	C64	C65	C66	C61	0.9(4)
C52	C39	C40	C41	-178.48(14)	C28	C27	C26	C25	-1.2(3)
C55	S4	C38	C37	0.64(13)	C72	C71	C70	C69	-2.2(3)
C55	S4	C38	C39	179.45(17)	C72	C67	C68	C69	-2.0(3)
C55	C60	C59	N2	179.21(15)	C12	C11	C18	C7	-179.61(15)
C55	C60	C59	C58	0.6(3)	C12	C11	C18	C17	-0.3(2)
C41	C42	C43	C54	-0.2(2)	C12	C13	C14	C15	-179.62(16)
C41	C42	C43	C44	-179.27(15)	C12	C13	C14	C17	0.2(2)
C62	C63	C64	C65	0.9(4)	C59	N2	C67	C68	104.1(2)
C62	C61	C66	C65	0.8(3)	C59	N2	C67	C72	-74.5(2)
C15	C14	C17	C18	179.94(15)	C59	N2	C61	C62	-23.7(3)
C15	C14	C17	C4	-1.2(2)	C59	N2	C61	C66	156.72(18)
C49	C48	C47	C54	-0.1(2)	C59	C58	C57	C56	2.2(3)

Table S9 Bond Lengths for **PTBT-O-NPh$_2$**

Atom	Atom	Length/Å	Atom	Atom	Length/Å
S4	O7	1.431(2)	C58	C59	1.412(5)
S4	O8	1.429(3)	C58	C57	1.381(5)
S4	C55	1.786(3)	C67	C72	1.370(5)
S4	C38	1.787(3)	C67	C68	1.377(5)
S1	O1	1.431(3)	C36	C35	1.391(5)
S1	O2	1.427(3)	C36	C31	1.380(5)
S1	C1	1.774(3)	C26	C27	1.382(5)
S1	C16	1.788(3)	C60	C59	1.418(4)
S2	O4	1.424(3)	C50	C49	1.439(5)
S2	O3	1.433(3)	C50	C51	1.401(5)
S2	C2	1.779(3)	C22	C21	1.387(5)
S2	C19	1.774(3)	C14	C13	1.428(4)
S3	O5	1.430(3)	C10	C11	1.397(5)
S3	O6	1.432(3)	C40	C41	1.433(5)
S3	C52	1.773(3)	C52	C51	1.366(5)
S3	C37	1.766(3)	C30	C29	1.389(5)
N2	C67	1.441(4)	C56	C37	1.450(5)
N2	C59	1.385(4)	C56	C57	1.391(5)
N2	C61	1.436(4)	C38	C37	1.339(5)
N1	C23	1.386(4)	C54	C47	1.429(5)
N1	C25	1.436(4)	C54	C43	1.416(5)
N1	C31	1.439(4)	C70	C71	1.386(6)
C23	C22	1.412(5)	C70	C69	1.376(6)
C23	C24	1.413(5)	C11	C18	1.430(5)
C25	C26	1.387(5)	C11	C12	1.434(5)

C25	C30	1.379(5)	C19	C24	1.367(4)
C34	C35	1.367(5)	C49	C48	1.344(6)
C34	C33	1.383(5)	C71	C72	1.379(5)
C55	C60	1.366(4)	C48	C47	1.425(6)
C55	C56	1.398(5)	C4	C3	1.398(5)
C2	C1	1.345(5)	C4	C5	1.431(5)
C2	C3	1.463(4)	C45	C44	1.380(6)
C17	C14	1.421(5)	C45	C46	1.374(6)
C17	C18	1.418(5)	C44	C43	1.403(5)
C17	C4	1.437(4)	C31	C32	1.384(5)
C15	C14	1.417(5)	C13	C12	1.347(5)
C15	C16	1.367(4)	C47	C46	1.404(6)
C7	C18	1.417(5)	C61	C66	1.384(5)
C7	C8	1.400(5)	C61	C62	1.388(5)
C7	C6	1.439(5)	C68	C69	1.390(6)
C9	C10	1.371(6)	C66	C65	1.379(5)
C9	C8	1.392(5)	C63	C62	1.386(5)
C39	C40	1.403(5)	C63	C64	1.378(6)
C39	C52	1.409(5)	C41	C42	1.354(5)
C39	C38	1.459(4)	C29	C28	1.373(6)
C20	C1	1.455(4)	C33	C32	1.377(5)
C20	C19	1.393(4)	C16	C3	1.404(4)
C20	C21	1.394(5)	C42	C43	1.429(5)
C53	C50	1.419(5)	C5	C6	1.349(5)
C53	C40	1.442(4)	C64	C65	1.381(6)
C53	C54	1.426(5)	C28	C27	1.382(6)

Table S10 Bond Angles for **PTBT-O-NPh$_2$**

Atom	Atom	Atom	Angle/˚	Atom	Atom	Atom	Angle/˚
O7	S4	C55	111.44(14)	C39	C40	C53	117.5(3)
O7	S4	C38	109.76(14)	C39	C40	C41	123.9(3)
O8	S4	O7	118.18(15)	C41	C40	C53	118.6(3)
O8	S4	C55	110.42(14)	C34	C35	C36	119.9(3)
O8	S4	C38	111.46(15)	C39	C52	S3	111.2(2)
C55	S4	C38	92.69(15)	C51	C52	S3	124.7(3)
O1	S1	C1	110.55(15)	C51	C52	C39	124.1(3)
O1	S1	C16	110.00(15)	C25	C30	C29	119.6(3)
O2	S1	O1	118.16(16)	C55	C56	C37	110.4(3)
O2	S1	C1	110.92(15)	C57	C56	C55	117.5(3)
O2	S1	C16	112.13(16)	C57	C56	C37	132.1(3)
C1	S1	C16	92.04(15)	C39	C38	S4	134.7(3)
O4	S2	O3	118.18(17)	C37	C38	S4	107.7(2)
O4	S2	C2	111.44(16)	C37	C38	C39	117.6(3)
O4	S2	C19	111.18(15)	C53	C54	C47	120.0(3)

O3	S2	C2	110.31(15)	C43	C54	C53	120.7(3)
O3	S2	C19	110.37(15)	C43	C54	C47	119.4(3)
C19	S2	C2	92.41(15)	C69	C70	C71	119.9(4)
O5	S3	O6	117.47(16)	C10	C11	C18	118.9(3)
O5	S3	C52	111.17(15)	C10	C11	C12	122.9(3)
O5	S3	C37	110.32(16)	C18	C11	C12	118.2(3)
O6	S3	C52	111.65(16)	C20	C19	S2	111.0(2)
O6	S3	C37	111.22(15)	C24	C19	S2	124.2(2)
C37	S3	C52	92.19(15)	C24	C19	C20	124.8(3)
C59	N2	C67	118.0(3)	C48	C49	C50	121.2(4)
C59	N2	C61	123.4(3)	C72	C71	C70	120.4(4)
C61	N2	C67	116.5(3)	C49	C48	C47	121.7(3)
C23	N1	C25	121.7(3)	C67	C72	C71	119.8(4)
C23	N1	C31	122.3(3)	C17	C18	C11	120.2(3)
C25	N1	C31	115.9(2)	C7	C18	C17	120.6(3)
N1	C23	C22	121.4(3)	C7	C18	C11	119.2(3)
N1	C23	C24	119.9(3)	C56	C37	S3	131.6(3)
C22	C23	C24	118.7(3)	C38	C37	S3	109.6(2)
C26	C25	N1	118.8(3)	C38	C37	C56	118.8(3)
C30	C25	N1	120.9(3)	C3	C4	C17	117.7(3)
C30	C25	C26	120.2(3)	C3	C4	C5	123.7(3)
C35	C34	C33	120.4(3)	C5	C4	C17	118.6(3)
C60	C55	S4	125.6(3)	C46	C45	C44	120.7(4)
C60	C55	C56	124.3(3)	C45	C44	C43	120.5(4)
C56	C55	S4	110.1(2)	C36	C31	N1	119.4(3)
C1	C2	S2	108.4(2)	C36	C31	C32	120.0(3)
C1	C2	C3	117.6(3)	C32	C31	N1	120.7(3)
C3	C2	S2	133.9(3)	C12	C13	C14	121.5(3)
C14	C17	C4	120.8(3)	C48	C47	C54	118.6(3)
C18	C17	C14	119.6(3)	C46	C47	C54	118.5(4)
C18	C17	C4	119.5(3)	C46	C47	C48	122.9(3)
C16	C15	C14	117.2(3)	C22	C21	C20	119.2(3)
C18	C7	C6	118.3(3)	C58	C57	C56	120.0(3)
C8	C7	C18	119.7(3)	C66	C61	N2	121.5(3)
C8	C7	C6	122.0(3)	C66	C61	C62	119.5(3)
C10	C9	C8	120.8(4)	C62	C61	N2	118.8(3)
C40	C39	C52	119.0(3)	C67	C68	C69	120.4(4)
C40	C39	C38	131.6(3)	C65	C66	C61	120.4(3)
C52	C39	C38	109.4(3)	C70	C69	C68	119.3(4)
C19	C20	C1	110.1(3)	C13	C12	C11	121.5(3)
C19	C20	C21	117.9(3)	C64	C63	C62	120.5(4)
C21	C20	C1	132.1(3)	C42	C41	C40	120.9(3)
C50	C53	C40	121.2(3)	C28	C29	C30	120.4(4)
C50	C53	C54	119.5(3)	C32	C33	C34	119.9(3)

C54	C53	C40	119.3(3)	C15	C16	S1	124.2(3)
C2	C1	S1	109.4(2)	C15	C16	C3	124.7(3)
C2	C1	C20	117.9(3)	C3	C16	S1	111.1(2)
C20	C1	S1	132.4(3)	C4	C3	C2	130.9(3)
C57	C58	C59	121.9(3)	C4	C3	C16	119.4(3)
C72	C67	N2	120.7(3)	C16	C3	C2	109.7(3)
C72	C67	C68	120.2(3)	C63	C62	C61	119.7(4)
C68	C67	N2	119.2(3)	C41	C42	C43	122.3(4)
C31	C36	C35	119.8(3)	C33	C32	C31	120.0(3)
C27	C26	C25	119.5(4)	C6	C5	C4	121.3(3)
C55	C60	C59	118.1(3)	C63	C64	C65	119.7(3)
C53	C50	C49	118.9(3)	C52	C51	C50	118.5(3)
C51	C50	C53	119.6(3)	C45	C46	C47	121.4(4)
C51	C50	C49	121.5(3)	C9	C8	C7	120.1(4)
N2	C59	C58	121.7(3)	C19	C24	C23	117.4(3)
N2	C59	C60	120.2(3)	C54	C43	C42	118.2(3)
C58	C59	C60	118.1(3)	C44	C43	C54	119.6(3)
C21	C22	C23	122.0(3)	C44	C43	C42	122.2(4)
C17	C14	C13	119.0(3)	C29	C28	C27	119.7(3)
C15	C14	C17	120.1(3)	C66	C65	C64	120.2(4)
C15	C14	C13	120.9(3)	C28	C27	C26	120.5(3)
C9	C10	C11	121.3(3)	C5	C6	C7	121.7(3)

Table S11 Torsion Angles for **PTBT-O-NPh$_2$**

A	B	C	D	Angle/˚	A	B	C	D	Angle/˚
S4	C55	C60	C59	-178.5(2)	C14	C17	C4	C3	-0.9(4)
S4	C55	C56	C37	4.5(3)	C14	C17	C4	C5	177.7(3)
S4	C55	C56	C57	-178.3(2)	C14	C15	C16	S1	-178.2(2)
S4	C38	C37	S3	178.01(16)	C14	C15	C16	C3	-0.3(5)
S4	C38	C37	C56	-3.8(4)	C14	C13	C12	C11	1.4(5)
S1	C16	C3	C2	-3.5(3)	C10	C9	C8	C7	1.2(6)
S1	C16	C3	C4	176.5(2)	C10	C11	C18	C17	-179.0(3)
S2	C2	C1	S1	177.73(16)	C10	C11	C18	C7	-1.0(5)
S2	C2	C1	C20	2.8(4)	C10	C11	C12	C13	178.0(3)
S2	C2	C3	C4	6.1(6)	C40	C39	C52	S3	-178.4(2)
S2	C2	C3	C16	-173.9(3)	C40	C39	C52	C51	-0.6(5)
S2	C19	C24	C23	-179.9(2)	C40	C39	C38	S4	1.3(6)
S3	C52	C51	C50	178.5(2)	C40	C39	C38	C37	-179.1(3)
O7	S4	C55	C60	-74.0(3)	C40	C53	C50	C49	-179.9(3)
O7	S4	C55	C56	106.8(2)	C40	C53	C50	C51	0.8(5)
O7	S4	C38	C39	70.9(4)	C40	C53	C54	C47	-179.0(3)
O7	S4	C38	C37	-108.7(2)	C40	C53	C54	C43	0.3(5)
O1	S1	C1	C2	109.5(3)	C40	C41	C42	C43	0.4(6)
O1	S1	C1	C20	-76.5(3)	C35	C34	C33	C32	-2.3(6)

O1	S1	C16	C15	69.0(3)	C35	C36	C31	N1	177.6(3)
O1	S1	C16	C3	-109.1(2)	C35	C36	C31	C32	-1.1(5)
O4	S2	C2	C1	-117.6(3)	C52	S3	C37	C56	-174.9(3)
O4	S2	C2	C3	58.1(4)	C52	S3	C37	C38	3.0(3)
O4	S2	C19	C20	118.0(2)	C52	C39	C40	C53	0.2(4)
O4	S2	C19	C24	-62.4(3)	C52	C39	C40	C41	179.4(3)
O8	S4	C55	C60	59.4(3)	C52	C39	C38	S4	179.4(3)
O8	S4	C55	C56	-119.8(2)	C52	C39	C38	C37	-1.0(4)
O8	S4	C38	C39	-61.9(4)	C30	C25	C26	C27	-1.0(5)
O8	S4	C38	C37	118.5(2)	C30	C29	C28	C27	-2.0(6)
O5	S3	C52	C39	109.2(2)	C56	C55	C60	C59	0.5(5)
O5	S3	C52	C51	-68.6(3)	C38	S4	C55	C60	173.5(3)
O5	S3	C37	C56	71.5(4)	C38	S4	C55	C56	-5.7(3)
O5	S3	C37	C38	-110.6(3)	C38	C39	C40	C53	178.2(3)
O3	S2	C2	C1	109.1(3)	C38	C39	C40	C41	-2.7(6)
O3	S2	C2	C3	-75.2(4)	C38	C39	C52	S3	3.2(3)
O3	S2	C19	C20	-108.8(2)	C38	C39	C52	C51	-179.0(3)
O3	S2	C19	C24	70.8(3)	C54	C53	C50	C49	0.3(5)
O6	S3	C52	C39	-117.5(2)	C54	C53	C50	C51	-179.0(3)
O6	S3	C52	C51	64.7(3)	C54	C53	C40	C39	179.4(3)
O6	S3	C37	C56	-60.7(4)	C54	C53	C40	C41	0.2(5)
O6	S3	C37	C38	117.2(3)	C54	C47	C46	C45	0.4(5)
O2	S1	C1	C2	-117.4(3)	C70	C71	C72	C67	-0.6(6)
O2	S1	C1	C20	56.5(4)	C19	S2	C2	C1	-3.7(3)
O2	S1	C16	C15	-64.6(3)	C19	S2	C2	C3	172.0(3)
O2	S1	C16	C3	117.3(2)	C19	C20	C1	S1	-173.5(3)
N2	C67	C72	C71	-177.6(3)	C19	C20	C1	C2	0.1(4)
N2	C67	C68	C69	177.3(4)	C19	C20	C21	C22	1.5(5)
N2	C61	C66	C65	175.8(3)	C49	C50	C51	C52	179.6(3)
N2	C61	C62	C63	-175.0(4)	C49	C48	C47	C54	1.9(5)
N1	C23	C22	C21	176.3(3)	C49	C48	C47	C46	-179.3(4)
N1	C23	C24	C19	-176.6(3)	C71	C70	C69	C68	-0.7(6)
N1	C25	C26	C27	175.4(3)	C48	C47	C46	C45	-178.5(4)
N1	C25	C30	C29	-175.5(3)	C72	C67	C68	C69	-1.4(6)
N1	C31	C32	C33	-178.9(3)	C18	C17	C14	C15	178.9(3)
C23	N1	C25	C26	115.2(4)	C18	C17	C14	C13	-0.8(5)
C23	N1	C25	C30	-68.4(4)	C18	C17	C4	C3	179.3(3)
C23	N1	C31	C36	126.2(3)	C18	C17	C4	C5	-2.2(5)
C23	N1	C31	C32	-55.2(4)	C18	C7	C8	C9	-0.9(5)
C23	C22	C21	C20	0.7(5)	C18	C7	C6	C5	-1.2(5)
C25	N1	C23	C22	-11.4(5)	C18	C11	C12	C13	-1.7(5)
C25	N1	C23	C24	167.6(3)	C37	S3	C52	C39	-3.6(3)
C25	N1	C31	C36	-51.8(4)	C37	S3	C52	C51	178.6(3)
C25	N1	C31	C32	126.9(3)	C37	C56	C57	C58	174.3(3)

C25	C26	C27	C28	-0.3(6)	C4	C17	C14	C15	-1.0(5)
C25	C30	C29	C28	0.6(6)	C4	C17	C14	C13	179.3(3)
C34	C33	C32	C31	1.9(5)	C4	C17	C18	C7	2.4(5)
C55	S4	C38	C39	-175.1(3)	C4	C17	C18	C11	-179.6(3)
C55	S4	C38	C37	5.3(3)	C4	C5	C6	C7	1.4(6)
C55	C60	C59	N2	176.5(3)	C45	C44	C43	C54	0.6(6)
C55	C60	C59	C58	-3.8(5)	C45	C44	C43	C42	-178.7(4)
C55	C56	C37	S3	177.3(3)	C44	C45	C46	C47	-0.2(6)
C55	C56	C37	C38	-0.5(4)	C31	N1	C23	C22	170.8(3)
C55	C56	C57	C58	-2.2(5)	C31	N1	C23	C24	-10.2(5)
C2	S2	C19	C20	3.9(3)	C31	N1	C25	C26	-66.9(4)
C2	S2	C19	C24	-176.5(3)	C31	N1	C25	C30	109.5(4)
C17	C14	C13	C12	-0.1(5)	C31	C36	C35	C34	0.7(5)
C17	C4	C3	C2	-177.8(3)	C47	C54	C43	C44	-0.5(5)
C17	C4	C3	C16	2.1(5)	C47	C54	C43	C42	178.9(3)
C17	C4	C5	C6	0.3(5)	C21	C20	C1	S1	5.5(6)
C15	C14	C13	C12	-179.8(3)	C21	C20	C1	C2	179.0(3)
C15	C16	C3	C2	178.4(3)	C21	C20	C19	S2	177.9(2)
C15	C16	C3	C4	-1.6(5)	C21	C20	C19	C24	-1.7(5)
C9	C10	C11	C18	1.3(5)	C57	C58	C59	N2	-176.2(3)
C9	C10	C11	C12	-178.4(3)	C57	C58	C59	C60	4.1(5)
C39	C40	C41	C42	-179.7(3)	C57	C56	C37	S3	0.7(6)
C39	C52	C51	C50	1.0(5)	C57	C56	C37	C38	-177.1(3)
C39	C38	C37	S3	-1.7(4)	C61	N2	C67	C72	-100.5(4)
C39	C38	C37	C56	176.5(3)	C61	N2	C67	C68	80.8(4)
C20	C19	C24	C23	-0.3(5)	C61	N2	C59	C58	17.0(5)
C53	C50	C49	C48	-0.3(5)	C61	N2	C59	C60	-163.4(3)
C53	C50	C51	C52	-1.1(5)	C61	C66	C65	C64	0.1(6)
C53	C40	C41	C42	-0.6(5)	C68	C67	C72	C71	1.1(5)
C53	C54	C47	C48	-1.8(5)	C66	C61	C62	C63	1.3(6)
C53	C54	C47	C46	179.3(3)	C69	C70	C71	C72	0.4(6)
C53	C54	C43	C44	-179.8(3)	C12	C11	C18	C17	0.7(5)
C53	C54	C43	C42	-0.5(5)	C12	C11	C18	C7	178.7(3)
C1	S1	C16	C15	-178.2(3)	C63	C64	C65	C66	-0.6(6)
C1	S1	C16	C3	3.7(3)	C41	C42	C43	C54	0.1(6)
C1	C2	C3	C4	-178.6(3)	C41	C42	C43	C44	179.4(4)
C1	C2	C3	C16	1.5(4)	C29	C28	C27	C26	1.8(6)
C1	C20	C19	S2	-2.9(3)	C33	C34	C35	C36	1.0(6)
C1	C20	C19	C24	177.4(3)	C16	S1	C1	C2	-2.7(3)
C1	C20	C21	C22	-177.4(3)	C16	S1	C1	C20	171.2(3)
C67	N2	C59	C58	179.9(3)	C16	C15	C14	C17	1.5(5)
C67	N2	C59	C60	-0.4(5)	C16	C15	C14	C13	-178.7(3)
C67	N2	C61	C66	-113.0(4)	C3	C2	C1	S1	1.2(4)
C67	N2	C61	C62	63.2(4)	C3	C2	C1	C20	-173.7(3)

C67	C68	C69	C70	1.2(6)	C3	C4	C5	C6	178.8(3)
C36	C31	C32	C33	-0.2(5)	C62	C61	C66	C65	-0.4(6)
C26	C25	C30	C29	0.8(5)	C62	C63	C64	C65	1.5(7)
C60	C55	C56	C37	-174.7(3)	C5	C4	C3	C2	3.7(6)
C60	C55	C56	C57	2.5(5)	C5	C4	C3	C16	-176.4(3)
C50	C53	C40	C39	-0.4(5)	C64	C63	C62	C61	-1.9(6)
C50	C53	C40	C41	-179.6(3)	C51	C50	C49	C48	179.0(3)
C50	C53	C54	C47	0.7(5)	C46	C45	C44	C43	-0.3(6)
C50	C53	C54	C43	-179.9(3)	C8	C7	C18	C17	178.8(3)
C50	C49	C48	C47	-0.8(6)	C8	C7	C18	C11	0.8(5)
C59	N2	C67	C72	95.4(4)	C8	C7	C6	C5	179.3(4)
C59	N2	C67	C68	-83.3(4)	C8	C9	C10	C11	-1.4(6)
C59	N2	C61	C66	50.2(5)	C24	C23	C22	C21	-2.7(5)
C59	N2	C61	C62	-133.6(4)	C43	C54	C47	C48	178.8(3)
C59	C58	C57	C56	-1.1(5)	C43	C54	C47	C46	0.0(5)
C22	C23	C24	C19	2.4(5)	C6	C7	C18	C17	-0.8(5)
C14	C17	C18	C7	-177.5(3)	C6	C7	C18	C11	-178.8(3)
C14	C17	C18	C11	0.5(5)	C6	C7	C8	C9	178.7(3)

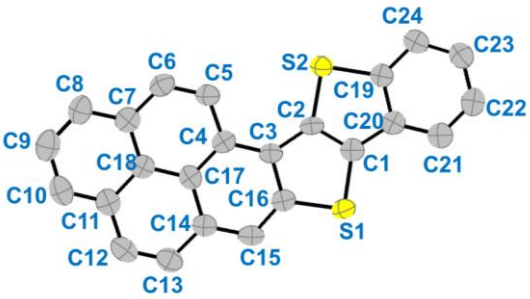

Figure S24 X-ray structure of **PTBT-H**

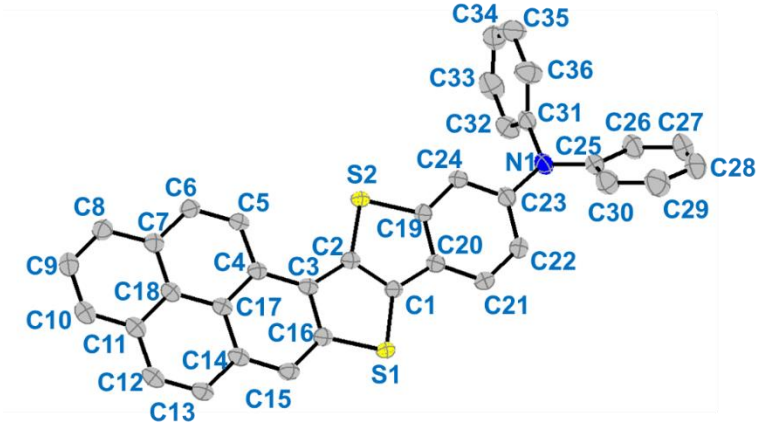

Figure S25 X-ray structure of **PTBT-NPh$_2$**

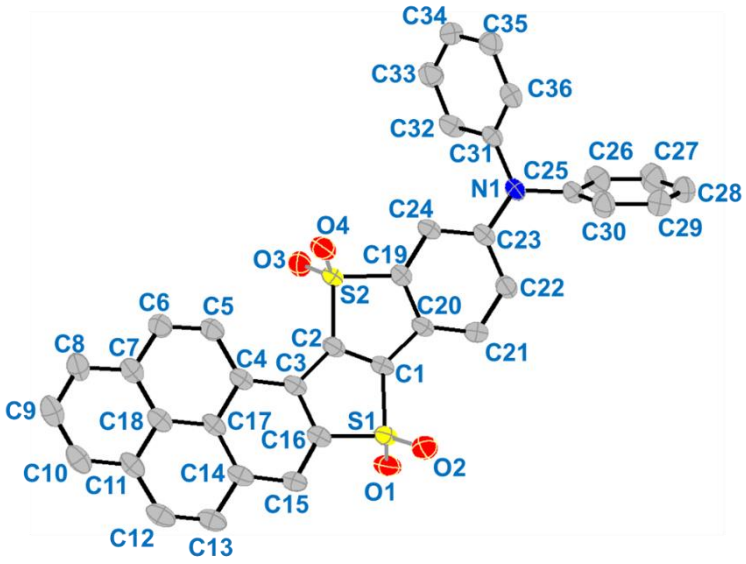

Figure S26 X-ray structure of **PTBT-O-NPh$_2$**

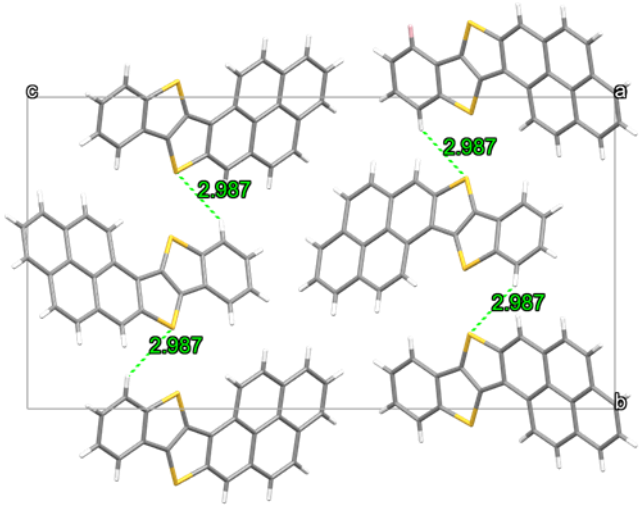

Figure S 27 Packing diagram of PTBT-H.

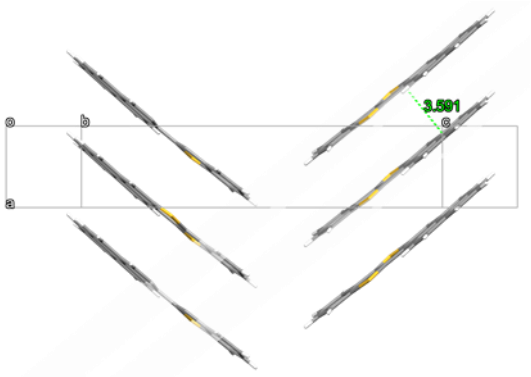

Figure S 28 Packing diagram of PTBT-H.

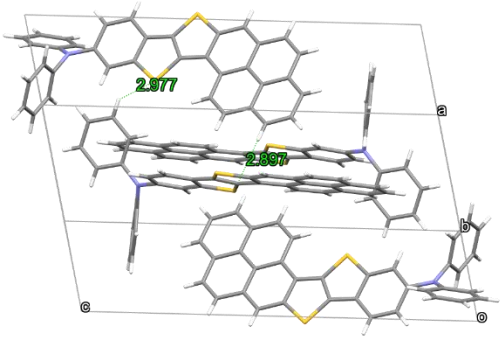

Figure S 29 Packing diagram of PTBT-NPh$_2$.

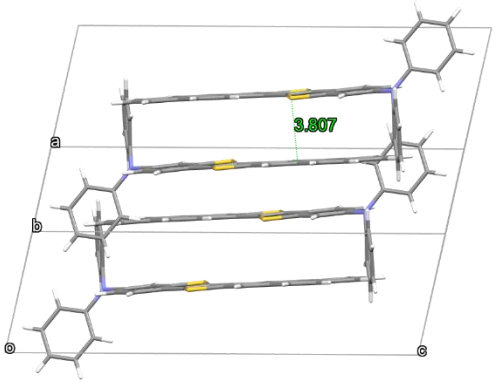

Figure S 30 Packing diagram of PTBT-NPh$_2$.

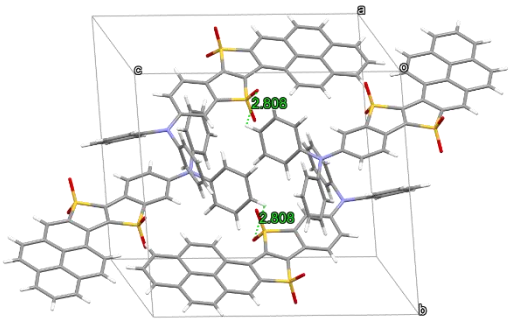

Figure S 31 Packing diagram of PTBT-O-NPh$_2$.

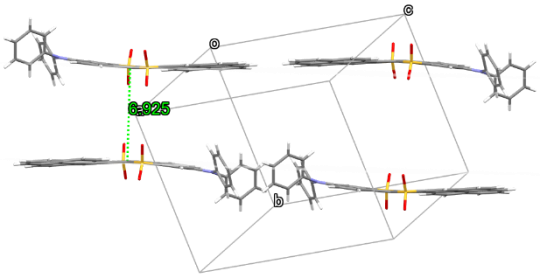

Figure S 32 Packing diagram of PTBT-O-NPh$_2$.

5. Photophysical measurements

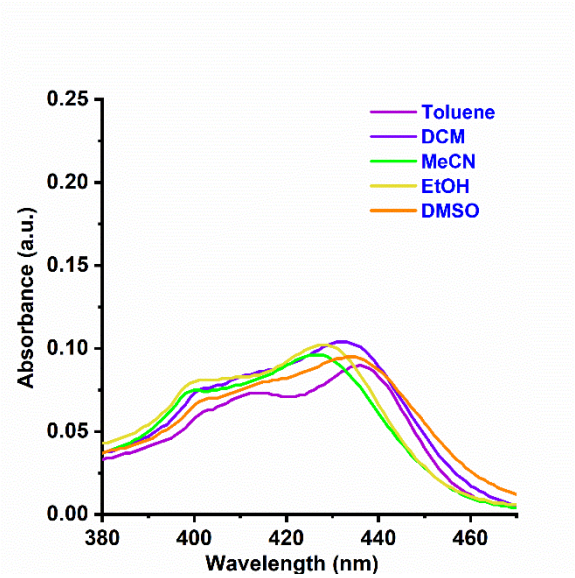

Figure S33 UV-vis absorption spectra of **PTBT-NPh$_2$** in different solvents at 8.0×10^{-5} mol/L

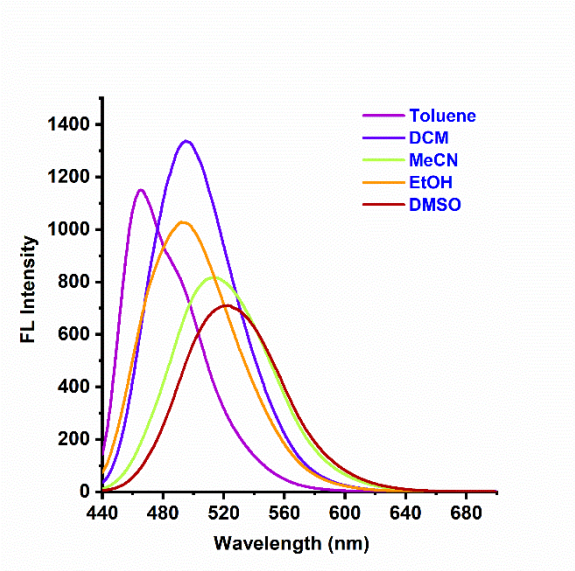

Figure S34 Fluorescence emission spectra of **PTBT-NPh$_2$** in different solvents at 8.0×10^{-5} mol/L

(ex = 430nm)

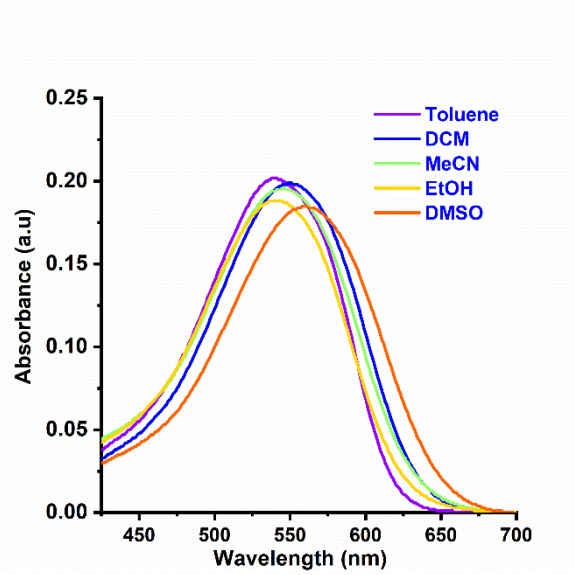

Figure S35 UV-vis absorption spectra of **PTBT-O-NPh$_2$** in different solvents at 1.0×10^{-5} mol/L

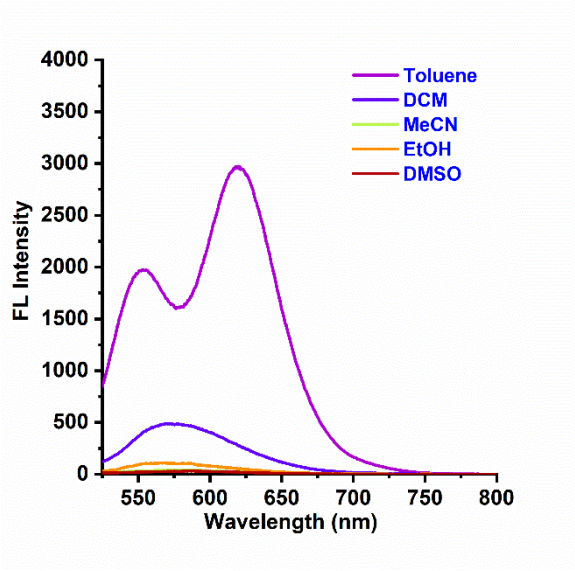

Figure S36 Fluorescence emission spectra of **PTBT-O-NPh$_2$** in different solvents at 1.0×10^{-5} mol/L (ex = 500 nm)

Table S12 Photophysical Data for **PTBT-NPh$_2$** and **PTBT-O-NPh$_2$**

Comp.	Solvent	λ_{abs}/nm	$\varepsilon/10^4 M^{-1}cm^{-1}$	λ_{em}/nm	Φ_F	τ/ns	Stokes shift/cm^{-1}	Brightness ($\varepsilon*\Phi_F$)
PTBT-NPh$_2$	Toluene	436	0.11	465	0.57	1.01	1430	641
	CH_2Cl_2	432	0.13	495	0.84	1.64	2946	1092
	THF	432	0.12	491.5	0.95	2.03	2802	812.71
	EtOAc	433	0.11	495.5	0.73	1.66	2913	803
	DMSO	435	0.12	523	0.95	1.28	3868	1129
	EtOH	428	0.13	492	0.62	2.03	3039	790
	MeOH	433	0.12	493	0.51	1.66	2811	612
PTBT-O-NPh$_2$	Toluene	540	2.02	552	0.64	4.27	403	12736
	CH_2Cl_2	550	1.99	572	0.032	5.06	699	640
	EtOAc	544	1.95	564	0.026	4.11	652	507
	THF	541	1.94	562.5	0.027	4.15	706.5	531.56
	DMSO	560	1.85	586.5	0.007	1.33	806	135
	EtOH	541	1.88	581.5	0.003	2.22	1287	54
	MeOH	543	1.86	583	0.002	2.04	1264	37

6. Confocal Imaging

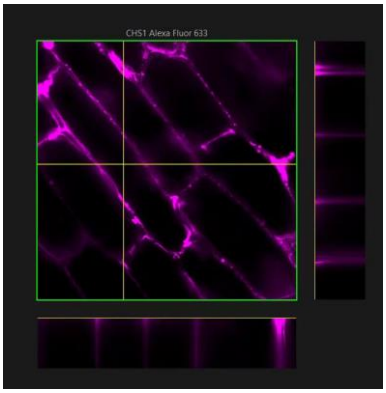

Figure S37 Photostability analysis of **DiD**

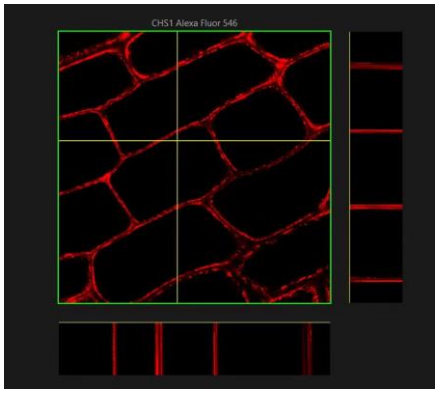

Figure S38 Photostability analysis of **PTBT-O-NPh2**

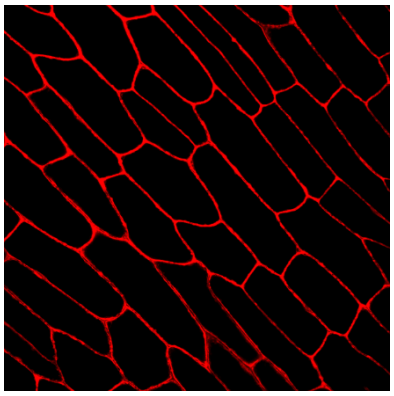

Figure S39 Imaging of onion inner epidermal cells after staining 48 h.

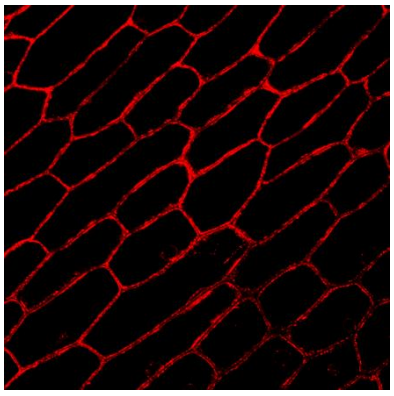

Figure S40 Imaging of onion inner epidermal cells after staining 120 h.

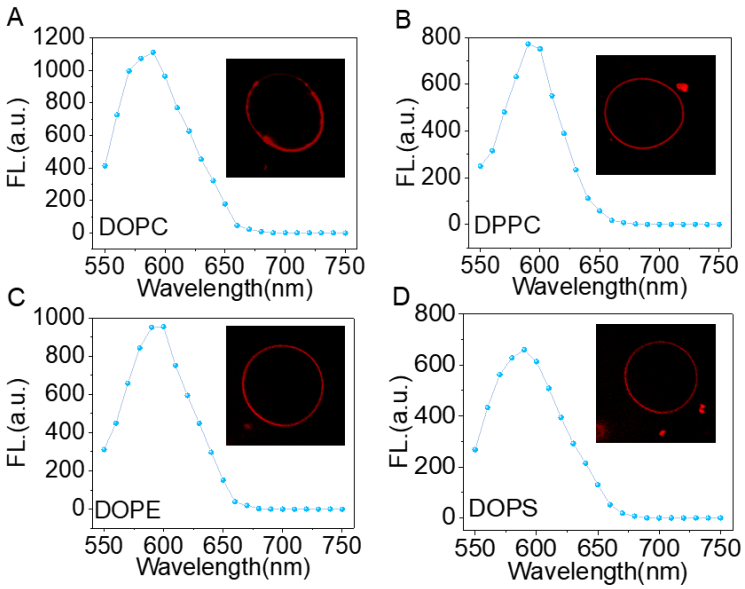

Figure S41 In-situ spectra and confocal imaging of **PTBT-O-NPh$_2$** in different MLVs.

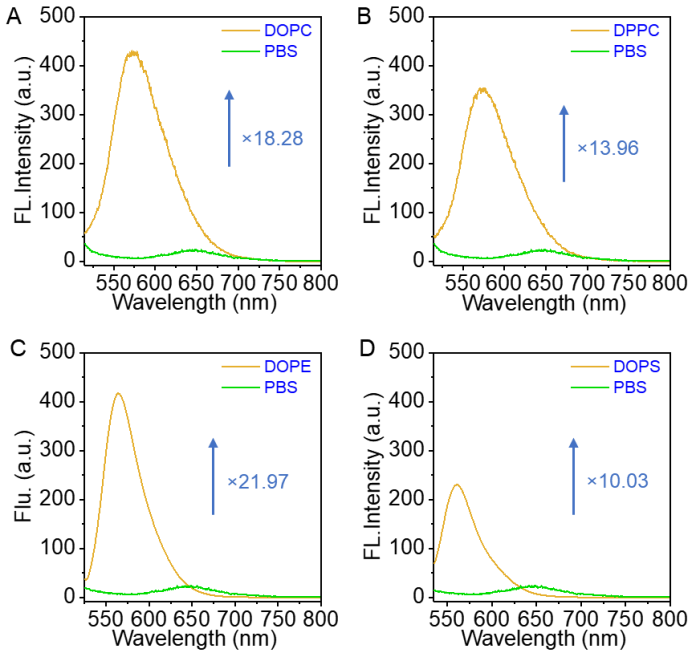

Figure S42 Responsiveness of **PTBT-O-NPh$_2$** to different phospholipids (DOPC, DPPC, DOPE, DOPS).

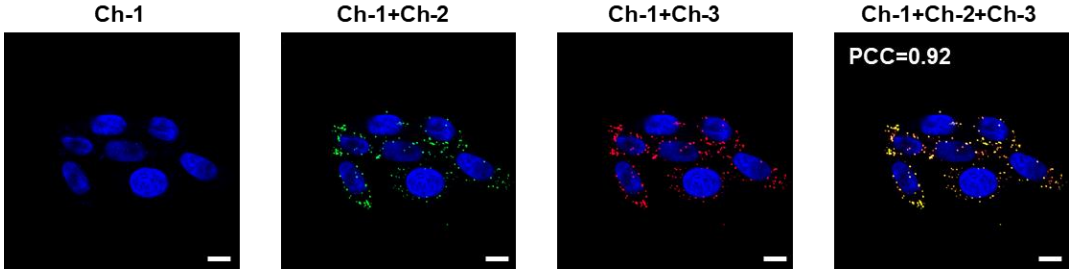

Figure S43 Confocal images of HeLa cells incubated with **PTBT-O-NPh$_2$** (10 μM), **hochest 33342** (5 μM), and **Bodipy 493/503** (2.5 μM). PCC: Pearson's correlation coefficient. Scale bar: 10 μm.

Ch-1: **hochest 33342**, λex =405 nm, λem =420-450 nm; Ch-2: **Bodipy 493/503**, λex =473 nm, λem =500-530 nm; Ch-3: **PTBT-O-NPh$_2$**, λex =543 nm, λem =550-650 nm.

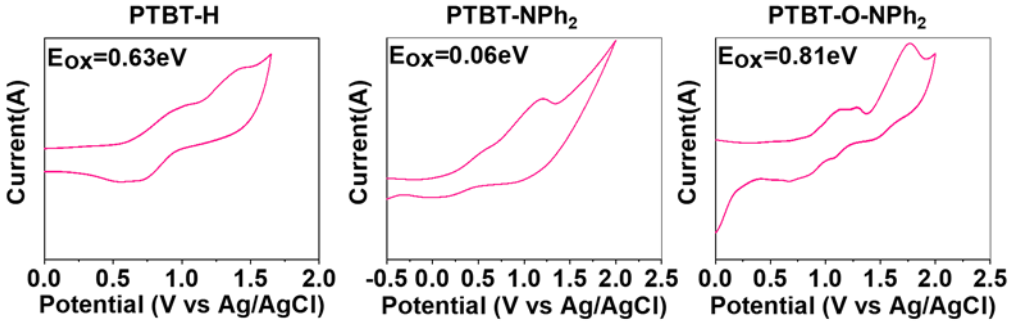

Figure S44 Cyclic voltammetry curves of compound **PTBT-H**, **PTBT-NPh$_2$** and **PTBT-O-NPh$_2$** at the scanning speed under 100 mV.